

Masanori Takahashi · Kenichi Sato · Tadashi Nomura
Noriko Osumi

Manipulating gene expressions by electroporation in the developing brain of mammalian embryos

Accepted in revised form: 1 April 2002

Abstract One of the goals of developmental neuroscience in the post-genomic era is to clarify functions of a huge number of anonymous genes of which only DNA sequences are identified. More convenient methods for genetic manipulation in vertebrates, especially mammals, could help us to identify functions of the novel genes. Here we introduce a novel gene transfer technology using electroporation (EP), which is a simple and powerful strategy for genetic analysis. We have applied this method to cultured mammalian embryos in order to understand the function of specific genes in the developing brain. We have also performed EP in developing fetuses *in utero* guided by ultrasound image. The combination of these techniques in addition to analysis of genetic mutants will clarify functions of individual genes, gene interactions, and the molecular mechanisms underlying the brain development.

Key words mammalian brain · electroporation · whole-embryo culture · *in utero* manipulation · ultrasound guided manipulation

Introduction

Recent studies have shown that molecular mechanisms which govern compartmentalization and neuronal differentiation are phylogenically conserved among a variety of vertebrate species (Puelles and Rubenstein, 1993; Inoue et al., 2001b). However, each vertebrate species has specific brain structures as a result of adaptation to

the environment. For example, mammals developed the six-layered neocortex for processing numerous environmental stimuli, while a similar structure was developed in the avian optic tectum as a visual center (La Vail and Cowan, 1971). One of the important issues in developmental neurobiology is how genetic mechanisms control the development of such species-specific brain structures. Although genome projects and transcriptome analyses may give us clues to identify the large number of genes expressed during mammalian brain development, the task we face in the post-genomic research era is to analyze functions and interactions of these novel genes.

For a better understanding of the molecular basis for mammalian brain development *in vivo*, we need to manipulate gene expression in mammalian embryos and fetuses. Introduction of exogenous genes into embryos and targeting of given genes by homologous recombination are conventional and standard techniques to analyze gene function. However, several problems need to be overcome for strategies to succeed. First, regulatory elements which control expression of a gene of interest in a spatio-temporal manner during development are not always accessible to genetic manipulation by conventional techniques. Secondly, embryonic lethality of some mutations precludes investigation of gene function at later stages of development. Recently, techniques for conditional gene targeting and gene activation have been designed using the Cre/LoxP system or other genetic tools (see review by Porter, 1998). These methods have overcome some difficulties of conventional gene manipulation. However, a severe limitation of these systems is that much time and labor are needed to generate the transgenic animals upon which these systems rely.

Embryo culture systems have opened the way to investigate mammalian development. For post-implantation embryos, whole-embryo culture (WEC) is the most popular method (Cockroft, 1990; New, 1990; Morriss-

M. Takahashi¹ · K. Sato² · T. Nomura¹ · N. Osumi¹ (✉)

¹Department of Developmental Neurobiology, ²Department of Neurosurgery, Tohoku University Graduate School of Medicine, 2-1, Seiryomachi, Aoba-ku, Sendai 980-8575, Japan

e-mail: osumi@mail.cc.tohoku.ac.jp

Tel: +81 22 717 8201, Fax: +81 22 717 8205

Kay, 1993). Several surgical manipulations such as cell labeling (Serbedzija et al., 1990; Matsuo et al., 1993), cell grafting (Osumi-Yamashita et al., 1997; Kinder et al., 2000), and injection of antisense-oligonucleotides (Augustine et al., 1993) have been used in conjunction with mammalian WEC as well as in other vertebrate species (Heasman et al., 1991; 1994). However, this technique is not applicable for embryos at later stages because the placenta does not develop *in vitro*. In older mammalian embryos, *in utero* and *ex utero* manipulations are used to inject virus vectors for misexpression of genes (Muneoka et al., 1990; Papaioannou, 1990; Kagayama et al., 1996). *In utero* manipulation guided by ultrasound biomicroscope (UBM) has been used to inject virus solution (Gaiano et al., 2000) and to transplant cells (Olsson et al., 1997; Liu et al., 1998; Turnbull, 2000; Wichterle et al., 2001) into specific regions of the embryo.

Recently, introduction of exogenous genes by electroporation (EP) has proved to be a powerful tool, especially for avian embryologists (Muramatsu et al., 1997). We have adopted EP together with *in utero* manipulation of mammalian embryos/fetuses. Here we show the results of two gene transfer systems, using EP to introduce exogenous genes to the developing brain of rodent embryos or fetuses. We introduce a method that combines WEC with EP and *in utero* manipulation with EP that is guided by ultrasound imaging. We prefer to use rat embryos for *in vitro* manipulations because both their body size and litter size (number of embryos within one pregnant animal) are bigger than mice. The methods shown here are of course applicable for mouse embryos and fetuses. We believe the spatio-temporal targeting of these methods will provide more information on specific genetic interaction than can be ascertained from analysis of traditional knock-out or transgenic rodents alone.

Electroporation into cultured rat embryos

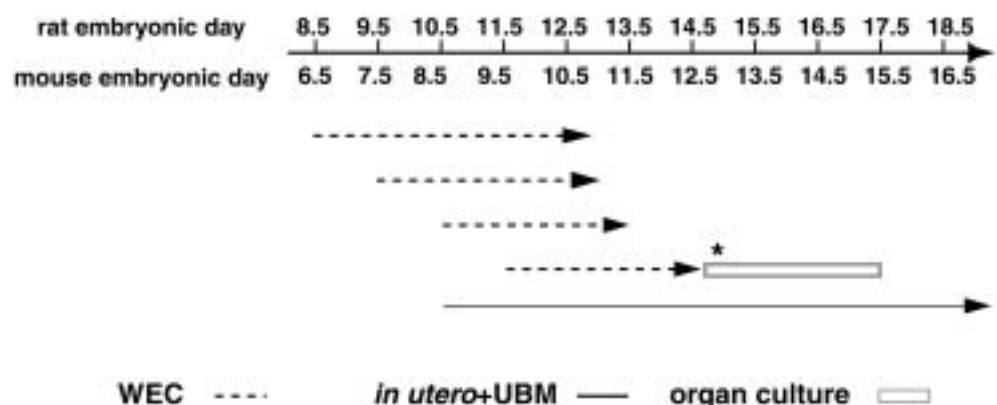
The *in ovo* electroporation (EP) method established originally by Muramatsu et al. (1997) has been widely used

in chick embryos for analyses of gene function in a variety of developmental events such as brain patterning and neural crest formation (Yasugi and Nakamura, 2000; Nakamura and Funahashi, 2001; Endo et al., 2002). We applied EP to rodent embryos in WEC to study the mechanism of mammalian brain development (see also Inoue et al., 2001a; Inoue and Krumlauf, 2001; Osumi and Inoue, 2001; Swartz et al., 2001; Takahashi and Osumi, 2002). This method leads to a high efficiency of exogenous gene expression in target tissues without tissue damage due to the use of square pulses for the electroporation. Expression of exogenous genes is transient but commences more quickly than expression mediated by virus vectors. Moreover, the strategy is safer than experiments using virus vectors. Here we show a further application of WEC + EP aimed at revealing genetic interactions in the developing rat hindbrain.

Methods for EP into cultured rat embryos

Our detailed procedures of EP + WEC have previously been described (Osumi and Inoue, 2001). WEC is applicable to E9.0–14.0 rat embryos (corresponding to E7.0–12.0 mouse embryos; Fig. 1); the growth of mammalian embryos at later stages depends on enough nutrients being provided through the placenta *in vivo*, but as mentioned, the placenta does not grow *in vitro*. Here we use EP E11.5 rat embryos, which are subsequently cultured for 1 day prior to expression and function analysis. For culture, the uterus is isolated from anaesthetised females; littermate embryos within the yolk sac with the placenta intact are dissected out and placed in sterile Tyrode's solution where the yolk sac is opened. After a 2-hour preculture in medium (100% rat serum (Charles River Japan, Inc) with 2 mg/ml glucose and antibiotics) the embryos were transferred into a chamber bordered on two sides by electrodes (8 × 20 mm electrodes and 20 mm distance between electrodes; Unique Medical Imada, Miyagi, Japan) which is filled with Tyrode's solution. A solution of 0.25 µl of plasmid DNA dissolved in phosphate buffered saline (PBS) at 5 mg/ml (with

Fig. 1 Time course showing applicable periods for various manipulations and gene transfer into mammalian embryos using EP. Asterisk indicates the period in which telencephalon dissected from cultured embryos can further be cultured in organ culture system for 3 days (T.N. and N.O; unpublished data). UBM: Ultrasound Biomicroscope.



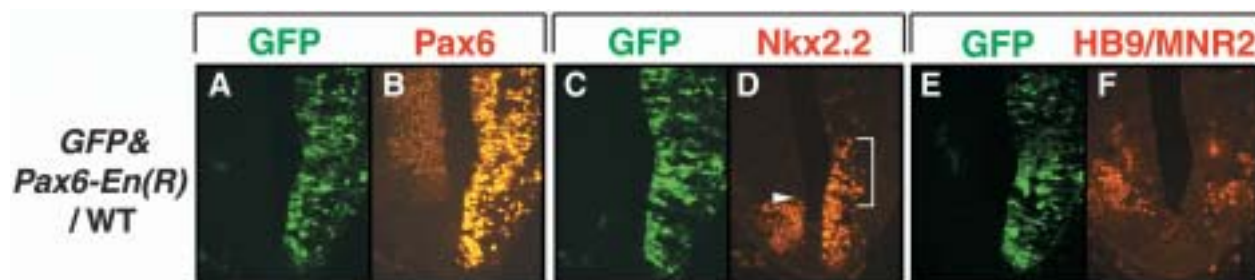


Fig. 2 Loss-of-function study by introduction of dominant-negative *Pax6* construct in cultured mammalian embryos. (A-F) *Pax6* dominant negative form, *Pax6-En(R)*, fused with *Drosophila engrailed* repressor domain was transfected into the hindbrain of early E11.5 (somite 22) wild-type rat embryo together with GFP reporter construct. These embryos were cultured for 24 hours after EP. GFP fluorescence and antibody staining were performed. Sets of two panels indicate double images of the same

section. (A, B) *Pax6-En(R)* fusion protein is detected by an antibody which recognizes the paired domain of Pax6. A very high degree of overlapping expression is observed between the electroporated Pax6 and GFP protein. Endogenous Pax6 protein is expressed in both sides. (C, D) *Pax6-En(R)* induced expansion of Nkx2.2 domain (bracket in D). (E, F) The numbers of HB9/MNR2 positive somatic motor neurons reduce due to indirect inhibition of Pax6 function.

0.05% Fast Green; Sigma Chemical Co., St. Louis, MO) is injected into the embryo's hindbrain with fine glass needles (outer diameter = 1 mm, inner diameter = 0.58 mm, length = 100 mm; B100-58-10; Sutter Instrument Co., Novato, CA). Immediately, square pulses (50 msec, 5 pulses at 1second intervals, 70 V, five times) are sent through the chamber using an electroporator (CUY21; NEPPA GENE, Tokyo, Japan). The embryos are returned to the culture medium and incubated at 37°C for one day. By using a general expression vector of one of CMV (cytomegalo virus), beta-actin, or EF-1 (elongation factor-1) promoters and changing direction and shape of electrodes, transgenes are introduced directly into specific brain regions where they are transiently expressed.

Loss of gene function study in cultured mammalian embryos

It has been reported that overexpression of dominant negative forms of a gene induces a loss-of-function phenotype in brain development (Akamatsu et al., 1999). Here, we show analyses on *Pax6* gene function in specification of ventral motor neurons and interneurons in the rodent hindbrain. To clarify gene cascades controlled by *Pax6*, we electroporated the truncated form of *Pax6* combined with *Drosophila engrailed* repressor domain (Yamasaki et al., 2001) into the hindbrain of cultured rat embryos. Together with co-transfected GFP gene product, used as an EP marker (Fig. 2A), strong expression of *Pax6-En(R)* protein was detected in the electroporated side (Fig. 2B). In the side where *Pax6-En(R)* was expressed, upregulation of Nkx2.2 was seen (bracket in Fig. 2D). Additionally, the number of HB9/MNR2 positive somatic motor (SM) neurons decreased (Fig. 2F). It should be noted that this expansion of Nkx2.2 domain and the decrease of SM neurons re-

semble the phenotype of the *Pax6* homozygous mutant rat (left side in Fig. 4D; also reported in Ericson et al., 1997; Takahashi and Osumi, 2002). These results suggest that EP of a dominant-negative form of a gene is very convenient strategy to elucidate its spatio-temporal roles in brain development.

Here, the fact that Nkx2.2 expands in the presence of dominant negative Pax6 leads to a couple of important conclusions on neuronal specification in the ventral hindbrain. First, several lines of evidence suggest that Pax6 represses Nkx2.2 (Ericson et al., 1997; Briscoe et al., 2000; Mastick and Andrews, 2001; Muhr et al., 2001). Our new result strongly suggests that this repression is not direct in the hindbrain. For example, if Pax6 bound directly to *Nkx2.2* promoter to repress it, then the *Pax6-EnR* protein would also repress Nkx2.2. Instead, our result implies that Pax6 normally activates some other factor, which then acts more directly to repress Nkx2.2. Second, Nkx2.2 does not turn on in all regions containing the dominant negative Pax6, suggesting that other factors that activate Nkx2.2, or other factors that can also repress Nkx2.2 in the absence of Pax6, must be spatially limited in their function.

Recent studies reported that modified antisense oligonucleotides (Morpholino) efficiently suppress gene expression in zebrafish embryogenesis (Nasevicius and Ekker, 2000). Morpholinos have higher affinity for mRNA than general antisense oligonucleotides and can alter RNA splicing and inhibit mRNA translation (Summerton and Weller, 1997; Summerton, 1999; Ekker and Larson, 2001; Heasman, 2002). It should be noted that the structure of Morpholinos is stable and does not exhibit toxicity for cells and tissues. Misexpression of Morpholino has been shown to knock down gene expression and therefore gene function in chick (Kos et al., 2001; Tucker, 2001), *Xenopus* (Heasman et al., 2000), and sea urchin (Howard et al., 2001) embryos. To obtain

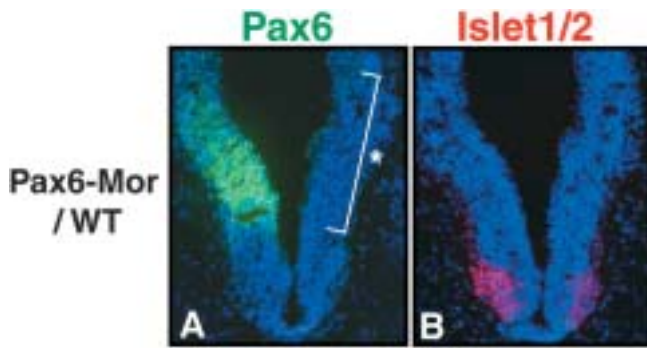


Fig. 3 Loss-of-function study by introduction of *Pax6* Morpholino oligonucleotides. (A, B) *Pax6* Morpholino oligonucleotides were transfected into the hindbrain of early E11.5 (somite 22) wild-type rat embryo. These embryos were cultured for 24 hours after EP. (A, B) Serial sections of the wild-type hindbrain electroporated with *Pax6*-Morpholino. (A) *Pax6* immunoreactivity is normally detected on the control side (green) but eliminated in the electroporated side, as indicated by *bracket*. (B) In the electroporated side, the number of *Islet1/2* positive motor neurons decreases. These sections are counterstained with DAPI (blue).

the loss-of-function phenotype of *Pax6*, we performed EP of *Pax6*-Morpholino into the rat hindbrain. We designed *Pax6*-Morpholino complementary to the sequence which covers the first 8 amino acids of mouse *Pax6* protein (5'-CACTCCGCTGTGACTGTTCTG-CATG-3'; underline indicates complementary sequences for the initiation codon). We injected approximately 0.25 μ l of Morpholino solution dissolved in 1 mM PBS with 0.05% Fast Green into the hindbrain of precultured rat embryos as described above. We electroporated using 5 square pulses (50 mseconds, 5 pulses at 1 second intervals, 65–70 V). Loss of endogenous expression of *Pax6* protein was observed in the electroporated side after several hours and up to at least 36 hours (Fig. 3A), indicating *Pax6*-Morpholino inhibited translation of *Pax6* mRNA. Also, the number of *Islet1/2* positive motor neurons decreased in the electroporated side (Fig. 3B), being a similar phenotype seen in the *Pax6* mutant hindbrain. These results suggest that EP of Morpholino is a useful and powerful technique for analysis of gene functions during mammalian brain development.

Gain-of-function study in cultured mutant embryos

Inoue et al. (2001a) have shown that ectopic cadherin-6 positive cells in the cortex side of wild-type mouse were sorted into the lateral ganglionic eminence (LGE) region where cadherin-6 is normally expressed. On the other hand, ectopic expression of cadherin-6 in the cortex of the *cadherin-6* mutant did not lead cell sorting to LGE side. We tested by EP in the *Pax6* mutant whether exoge-

nous *Pax6* can rescue the expression pattern of downstream genes that are altered in the *Pax6* mutant. As a result, *Nkx2.2* expression was repressed as seen in the wild type (bracket in Fig. 4D; see also Takahashi and Osumi, 2002). Previous studies reported that expression of *Wnt7b* and *En1* is missing in the *Pax6* mutant hindbrain (left side in Fig. 4F; Osumi et al., 1997; Burrill et al., 1997; Ericson et al., 1997; Osumi and Nakafuku, 1998). These molecules are normally expressed in *Pax6* positive neuroepithelial cells and their descendants, respectively. EP of *Pax6* into the *Pax6* mutant hindbrain recovered expression of *Wnt7b* (bracket in Fig. 4F) and *En1* (data not shown, see Takahashi and Osumi, 2002). These results suggest that *Pax6* acts as a positive regulator for *Wnt7b* and a negative regulator of *Nkx2.2*. Therefore, gain-of-function studies such as these combined with analysis of specific mutant mice may lead us to deepen our understanding of mechanisms which result in brain patterning.

Electroporation into embryos/fetuses developing *in utero*

To study long-term functions of genes involved in the brain development, another gene transfer system is needed. Such a system will allow embryos and fetuses to be experimentally manipulated throughout embryogenesis and then their development maintained up to delivery. Although the whole embryo culture system is very useful for the analysis of the molecular mechanisms of the developing mammalian brain, as mentioned earlier, the embryonic stages that can be studied are limited (Fig. 1).

Conventional *in utero* EP methods have been useful for the analysis of gene functions at later stages when the embryos are visible through the thin uterine wall (Saito and Nakatsuji, 2001; Tabata and Nakajima, 2001; Fukuchi-Shimogori and Grove, 2001). *In utero* manipulation of mouse embryos guided by ultrasound biomicroscope (UBM) established by Turnbull (2000) enables us to precisely manipulate embryos or fetuses even from early stages when they are veiled by the thicker uterine wall. Additionally, this method optimally maintains the development of the manipulated embryos/fetuses due to minimal invasion of pregnant mothers.

We have established a new gene transfer method using EP in combination with *in utero* ultrasound-guided operation to efficiently express exogenous genes. This method expands the application of *in utero* manipulation to earlier embryonic stages. The ultrasound-guided operation will assist in locating the injection of the DNA solution into a specific location of the embryo. Here we introduce *in utero* EP guided by UBM in rat embryos, but the technique is applicable to mouse embryos as well.

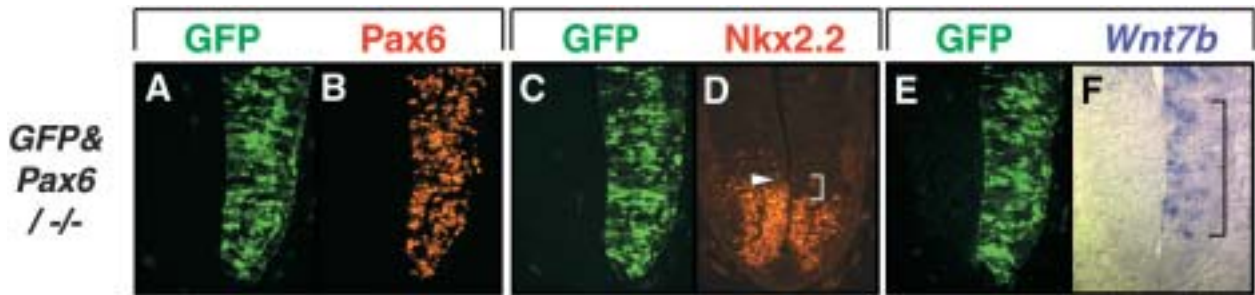


Fig. 4 Gain-of-function study by introduction of exogenous *Pax6*. (A-F) Wild-type form of *Pax6* was electroporated into the hindbrain of early E11.5 (somite 22) *Pax6* homozygous mutant rat embryo together with GFP reporter construct. These embryos were cultured for 24 hours after EP. Sets of two panels indicate double image of the same section. GFP fluorescence and antibody staining were performed except E and F (E, F) In E, GFP protein was detected by GFP antibody after *in situ* hybridization was per-

formed (F). (A, B) In the *Pax6* mutant, exogenous *Pax6* was only detected in the right side. (C, D) the expansion of *Nkx2.2* domain in the *Pax6* mutant hindbrain is repressed by exogenous *Pax6* (bracket in D). (E, F) In the ventral domain of the neural tube expressing *Pax6*, *Wnt7b* is coexpressed, while the expression is eliminated in the *Pax6* mutant (left side in F; see also Osumi et al., 1997). Exogenous *Pax6* induced *Wnt7b* expression (bracket in F).

Methods for *in utero* EP guided with UBM

In utero manipulation guided by UBM is as described by Turnbull (2000) with some modifications. After pregnant rats are anesthetized with sodium pentobarbital (0.7 mg/100 g body weight, injected intraperitoneally), the abdomen is shaved with a razor blade, and a 2-cm midline laparotomy is performed. A 100-mm diameter plastic petri dish with a 25-mm diameter hole sealed with a thin rubber membrane (Silastic L room temperature vulcanization (RTV) silicone rubber; Dow Corning) in the bottom center, is placed on the abdomen. The area of the skin that contacts the rubber is shaved carefully because hairs disrupt the seal of between the rubber membrane and the rat abdomen, leading to leakage of the solution in the Petri dish. The rat should be in a position which allows the abdomen to make good contact with the rubber membrane (Fig. 5A). Inappropriate abdominal positioning will restrict breathing of the animal and create excessive pressure on the uterus. The uterus is gently pulled from the abdomen through a slit in the rubber membrane into the petri dish filled with sterile PBS. We used a high-frequency ultrasound scanner (UBM; Paradigm Medical Industries, Salt Lake City, UT) to perform *in utero* embryo imaging. This imaging system is equipped with a high frequency (40–50 MHz) focused ultrasound transducer that is scanned mechanically to produce two-dimensional images in real time (Fig. 5A, C, D). While monitoring the images, an injection needle made of glass microcapillary pipettes (outer diameter = 1 mm, inner diameter = 0.5 mm, length = 100 mm; BF100-50-10; Sutter Instrument Co., Novato, CA) is inserted into the cerebral vesicle through the uterine wall, and plasmid DNA solution (2.5–5 $\mu\text{g}/\mu\text{l}$ with 0.05% Fast Green) is injected (Fig. 5A, D). The amount of the DNA solution for injection is approximately 1 μl , but varies according to the developmental stage of the em-

bryo. After injection of DNA, EP is performed using tweezer-type electrodes which consist of a pair of round platinum plates of 0.7 mm diameter (Unique Medical Imada, Miyagi, Japan) (Fig. 5B). Optimal conditions of electrical pulses vary according to developmental stages. We performed EP with 40–50 V, 50 mseconds, 5 pulses at 1 second intervals for E13.5 rat embryos. The sterile

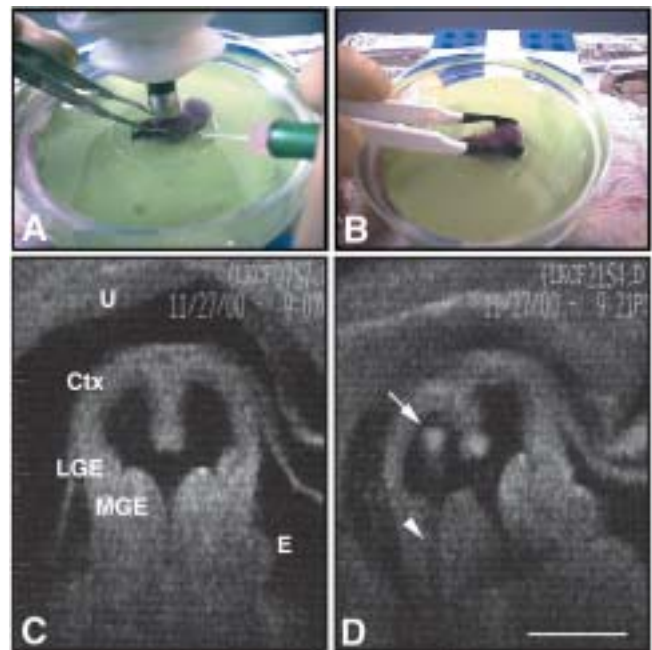


Fig. 5 Procedures for *in utero* EP and frontal section images of the E13.5 rat telencephalon through the UBM. (A) The uterus is held with the forceps and injected with a glass needle. (B) Electroporation with the tweezer-type electrode. All of these procedures are performed through the UBM imager. Before (C) and after (D) injection of DNA solution into the hemisphere. White arrow and arrowhead indicate injection needle and its acoustic shadow. E, eye; Ctx, cortex; LGE, lateral ganglionic eminence; MGE, medial ganglionic eminence; U, uterine wall. Bar = 1 mm.

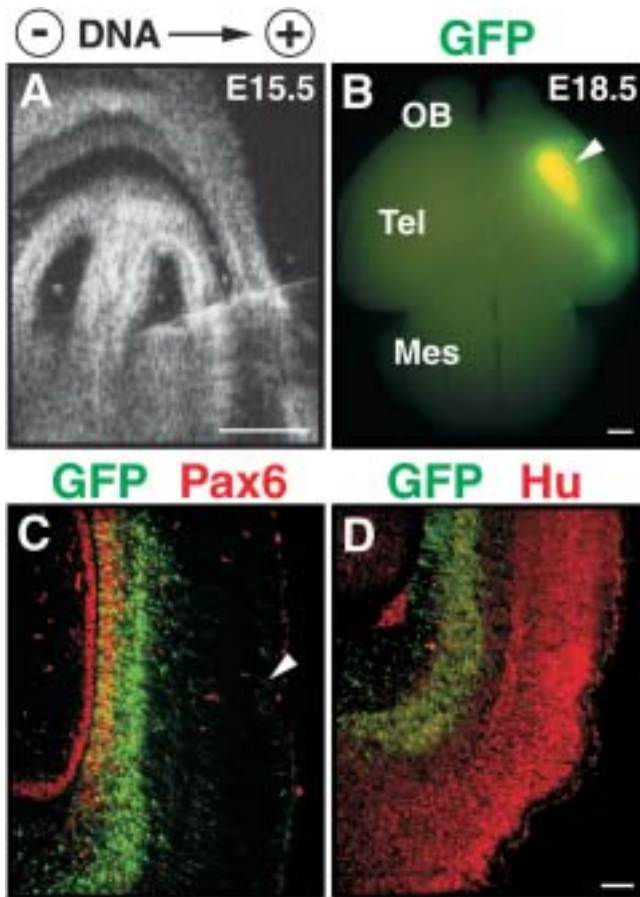


Fig. 6 Expression of the exogenous gene after *in utero* EP. (A) GFP expression vector was injected to the right lateral ventricle (LV) of E15.5 rat embryo by monitoring the image. DNA was electroporated toward the plus electrode. The direction of the electric field is indicated by + or -. (B) E18.5 whole brain of the same embryo. As expected, the expression of GFP was observed in the right telencephalon (white arrowhead). (C, D) Behavior of GFP-positive cells in E18.5 rat telencephalon electroporated at E15.5. Image of (D) is more ventral to that of (C). (C) GFP positive cells are green, and Pax6 are red. GFP positive cells coexpress Pax6 in the ventricular zone (yellow). Radial fibers extending toward the pial surface are also present (white arrowhead). (D) Immunostaining for a neuronal marker, Hu (red). In the whole layer except the ventricular zone, GFP positive cells coexpress Hu protein (yellow). Mes, mesencephalon; OB, olfactory bulb; Tel, telencephalon. Bar = 1 mm (A, B), 250 μm (C, D).

PBS in the petri dish should be changed after each EP procedure. The procedure should be completed within one hour. The survival rate of embryos is around 60%, but this also depends on the developmental stage of the embryo; the earlier embryos are more vulnerable.

Exogenous gene expression by ultrasound guided electroporation

A GFP expression vector, used as a marker for cells that incorporate the exogenous plasmid, was electroporated

to the ventricular zone of the lateral cortex in E15.5 rat embryo (Fig. 6A) by the methods described. Three days later, the expression of GFP was observed in the lateral side of the telencephalon (Fig. 6B). Furthermore, histological analysis showed that a large number of GFP positive cells were located in the ventricular zone, which is positive for Pax6 (Fig. 6C). GFP positive cells were also observed in the subventricular zone and the intermediate zone, where neuronal marker protein Hu is expressed (Fig. 6D). This finding suggests that these cells derived from the GFP-positive neuronal progenitor. Therefore, misexpression of genes of interest or introduction of dominant negative-constructs in the wild-type and mutant embryos could easily be performed using this method allowing for direct analysis of the gene of interest. Furthermore, as evidenced by the expression of GFP in Hu positive cells, this method can also be used to trace migration of neurons in normal and abnormal development (Tomioka et al., 2000; and T.N. and N.O., unpublished results).

Future applications

Gene transfer by EP combined with various manipulations of rodent embryos is a powerful tool for understanding molecular mechanisms of mammalian brain formation. Other applications of EP include analysis of enhancer regions by *in ovo* EP of reporter constructs driven by the enhancer regions in question (Itasaki et al., 1999; Muller et al., 2000; Sakamoto et al., 2000; Yasuda et al., 2000; Timmer et al., 2001). Therefore, introduction of these types of constructs or yeast artificial chromosome (YAC) clone including larger regulatory regions into cultured rodent embryos by EP may provide more quick and simple method to analyze or identify regulatory elements in the mouse genome.

WEC for rat embryos is restricted to E9.0–14.0 (corresponding to E7.0–12.0 in mouse embryos), and growth of embryos can be maintained for only 2–3 days after EP (Fig. 1). In contrast, we can maintain embryos electroporated *in utero* guided by UBM to full term and even analyze at postnatal or adult stages. Another technique available to enable analysis of development over a longer term than WEC/EP allows is organ culture combined with EP (Fig. 1; Tomioka et al., 2000; T.N. and N.O., unpublished data). For example, the whole telencephalon can be taken from cultured embryos, electroporated with a gene of interest, and cultured on the membrane for several days. In conclusion, we have tested various tools to explore mechanisms of brain development at the molecular level. EP combined with UBM, WEC, or organ culture are methods which allow analysis of mammalian specific brain formation, such as the establishment of the six-layered cortex and the subdivisions of the cortical areas.

Acknowledgements We thank Dr. D.H. Turnbull for kind advice on ultrasound-guided manipulation, Dr. V. van Heyningen for AD2.38 anti-Pax6 mouse monoclonal antibody, and Dr. Y. Wakamatsu for 16A11 anti-Hu mouse monoclonal antibody. We also thank Ms. Z. Altick and Dr. G. Mastick for critical reading of the manuscript. 40.2D6 anti-Islet1/2, 74.5A5 anti-Nkx2.2 and 81.5C10 anti-HB9/MNR2 mouse monoclonal antibodies were obtained from the Developmental Studies Hybridoma Bank (University of Iowa). This work was supported by Culture, Sports, Science and Technology (No. 10220209), CREST from Japanese Science and Technology Corporation, and a grant from Uehara Memorial Foundation (to N.O.).

References

- Akamatsu, W., Okano, H.J., Osumi, N., Inoue, T., Nakamura, S., Sakakibara, S., Miura, M., Matsuo, N., Darnell, R.B. and Okano, H. (1999) Mammalian ELAV-like neuronal RNA-binding proteins HuB and HuC promote neuronal development in both the central and the peripheral nervous systems. *Proc Natl Acad Sci USA* 96:9885–9890.
- Augustine, K., Liu, E.T. and Sadler, T.W. (1993) Antisense attenuation of Wnt-1 and Wn-3a expression in whole embryo culture reveals roles for these genes in craniofacial, spinal cord, and cardiac morphogenesis. *Develop Genet* 14:500–520.
- Briscoe, J., Pierani, A., Jessell, T.M. and Ericson, J. (2000) A homeodomain protein code specifies progenitor cell identity and neuronal fate in the ventral neural tube. *Cell* 101:435–445.
- Burrill, J.D., Moran, L., Goulding, M.D. and Saueressig, H. (1997) PAX2 is expressed in multiple spinal cord interneurons, including a population of EN1⁺ interneurons that require PAX6 for their development. *Development* 124:4493–4503.
- Cockroft, D.L. (1990) Do section and culture of post-implantation embryos. In: Copp, A.J. and Cockroft, D.L. (eds) *Mammalian Postimplantation Embryos: A Practical Approach*. IRL, Press, Oxford, pp 15–40.
- Ekker, S.C. and Larson, J.D. (2001) Morphant technology in model developmental systems. *Genesis* 30:89–93.
- Endo, Y., Osumi, N. and Wakamatsu, Y. (2002) Bimodal functions of Notch-mediated signaling are involved in neural crest formation during avian ectoderm development. *Development* 129:863–873.
- Ericson, J., Rashbass, P., Schedl, A., Brenner-Morton, S., Kawakami, A., van Heyningen, V., Jessell, T.M. and Briscoe, J. (1997) Pax6 controls progenitor cell identity and neuronal fate in response to graded Shh signaling. *Cell* 90:169–180.
- Fukuchi-Shimogori, T. and Grove, E.A. (2001) Neocortex patterning by the secreted signaling molecule FGF8. *Science* 294:1071–1074.
- Gaiano, N., Kohtz, J.D., Turnbull, D.H. and Fishell, G. (2000) A method for rapid gain-of-function studies in the mouse embryonic nervous system. *Nat Neurosci* 2:812–819.
- Heasman, J., Holwill, S. and Wylie, C.C. (1991) Fertilization of cultured *Xenopus* oocytes and use in studies of maternally inherited molecules. *Methods Cell Biol* 36:213–230.
- Heasman, J., Ginsberg, D., Geiger, B., Goldstone, K., Pratt, T., Yoshida-Noro, C. and Wylie, C. (1994) A functional test for maternally inherited cadherin in *Xenopus* shows its importance in cell adhesion at the blastula stage. *Development* 120:49–57.
- Heasman, J., Kofron, M. and Wylie, C. (2000) Beta-catenin signaling activity dissected in the early *Xenopus* embryo: a novel antisense approach. *Dev Biol* 222:124–134.
- Heasman, J. (2002) Morpholino oligos: making sense of antisense? *Dev Biol* 243:209–214.
- Howard, E.W., Newman, L.A., Oleksyn, D.W., Angerer, R.C. and Angerer, L.M. (2001) SpKrl: a direct target of beta-catenin regulation required for endoderm differentiation in sea urchin embryos. *Development* 128:365–375.
- Inoue, T. and Krumlauf, R. (2001) An impulse to the brain—using in vivo electroporation. *Nat Neurosci* 4(Suppl):1156–1158.
- Inoue, T., Tanaka, T., Takeichi, M., Chisaka, O., Nakamura, S. and Osumi, N. (2001a) Role of cadherins in maintaining the compartment boundary between the cortex and striatum during development. *Development* 128:561–569.
- Inoue, T., Nakamura, S. and Osumi, N. (2001b) Current topics in comparative developmental biology of vertebrate brains. *Neurosci Res* 39:371–376.
- Itasaki, N., Bel-Vialar, S. and Krumlauf, R. (1999) ‘Shocking’ developments in chick embryology: electroporation and in ovo gene expression. *Nat Cell Biol* 1:203–207.
- Kageyama, R., Ishibashi, M. and Moriyoshi, K. (1996) Gene delivery to the nervous system by direct injection of retroviral vector. In: Latchman (ed) *Genetic manipulation of the nervous system*. Academic Press, London, pp 135–148.
- Kinder, S.J., Tan, S.S. and Tam, P.P. (2000) Cell grafting and fate mapping of the early-somite-stage mouse embryo. *Methods Mol Biol* 135:425–437.
- Kos, R., Reedy, M.V., Johnson, R.L. and Erickson, C.A. (2001) The winged-helix transcription factor FoxD3 is important for establishing the neural crest lineage and repressing melanogenesis in avian embryos. *Development* 128:1467–1479.
- La Vail, J.H. and Cowan, W.M. (1971) The development of the chick optic tectum. I. Normal morphology and cytoarchitectonic development. *Brain Res* 28:391–419.
- Liu, A., Joyner, A.L. and Turnbull, D.H. (1998) Alteration of limb and brain patterning in early mouse embryos by ultrasound-guided injection of Shh-expressing cells. *Mech Dev* 75:107–115.
- Mastick, G.S. and Andrews, G.L. (2001) Pax6 regulates the identity of embryonic diencephalic neurons. *Mol Cell Neurosci* 17:190–207.
- Matsuo, T., Osumi-Yamashita, N., Noji, S., Ohuchi, H., Koyama, E., Myokai, F., Matsuo, N., Taniguchi, S., Doi, H., Iseki, S., Ninomiya, Y., Fujiwara, M., Watanabe, T. and Eto, K. (1993) A mutation in the Pax-6 gene in rat small eye is associated with impaired migration of midbrain crest cells. *Nat Genet* 3:299–304.
- Morriss-Kay, G.M. (1993) Postimplantation mammalian embryos. In: Stern, C.D. and Holland, P. (eds) *Essential Developmental Biology A Practical Approach*. IRL Press, Oxford, pp 55–66.
- Muhr, J., Andersson, E., Persson, M., Jessell, T.M. and Ericson, J. (2001) Groucho-mediated transcriptional repression establishes progenitor cell pattern and neuronal fate in the ventral neural tube. *Cell* 104:861–873.
- Muller, F., Albert, S., Blader, P., Fischer, N., Hallonet, M. and Strahle, U. (2000) Direct action of the nodal-related signal cyclops in induction of sonic hedgehog in the ventral midline of the CNS. *Development* 127:3889–3897.
- Muneoka, K., Wanek, N., Treviono, C. and Bryant, S.V. (1990) Exo utero surgery. In: Copp, A.J. and Cockroft, D.L. (eds) *Mammalian Postimplantation Embryos: A Practical Approach*. IRL, Press, Oxford, pp 41–59.
- Muramatsu, T., Mizutani, Y., Ohmori, Y. and Okumura, J. (1997) Comparison of three nonviral transfection methods for foreign gene expression in early chicken embryos in ovo. *Biochem Biophys Res Commun* 230:376–380.
- Nakamura, H. and Funahashi, J. (2001) Introduction of DNA into chick embryos by in ovo electroporation. *Methods* 24:43–48.
- Nasevicius, A. and Ekker, S.C. (2000) Effective targeted gene ‘knockdown’ in zebrafish. *Nat Genet* 26:216–220.
- New, D.A.T. (1990) Introduction. In: Copp, A.J. and Cockroft, D.L. (eds) *Mammalian Postimplantation Embryos: A Practical Approach*. IRL, Press, Oxford, pp 1–14.
- Olsson, M., Campbell, K. and Turnbull, D.H. (1997) Specification of mouse telencephalic and mid-hindbrain progenitors following heterotopic ultrasound-guided embryonic transplantation. *Neuron* 19:761–772.

- Osumi, N., Hirota, A., Ohuchi, H., Nakafuku, M., Iimura, T., Kuratani, S., Fujiwara, M., Noji, S. and Eto, K. (1997) *Pax-6* is involved in the specification of hindbrain motor neuron subtype. *Development* 124:2961–2972.
- Osumi, N. and Inoue, T. (2001) Gene transfer into cultured mammalian embryos by electroporation. *Methods* 24:35–42.
- Osumi, N. and Nakafuku, M. (1998) *Pax-6* is involved in specification of ventral cell types in the hindbrain. In: Uyemura, K., Kawamura, K. and Yazaki, T. (eds) *Neural Development: Keio Univ. Symposia for Life Science and Medicine Vol. 2*. Springer-Verlag, Tokyo, pp 1117–1124.
- Osumi-Yamashita, N., Kuratani, S., Ninomiya, Y., Aoki, K., Iseki, S., Chareonvit, S., Doi, H., Fujiwara, M., Watanabe, T. and Eto, K. (1997) Cranial anomaly of homozygous rSey rat is associated with a defect in the migration pathway of midbrain crest cells. *Dev Growth Differ* 39:53–67.
- Papaioannou, V.E. (1990) In utero manipulation. In: Copp, A.J. and Cockroft, D.L. (eds) *Mammalian Postimplantation Embryos: A Practical Approach*. IRL, Press, Oxford, pp 61–80.
- Porter, A. (1998) Controlling your losses: conditional gene silencing in mammals. *Trends Genet* 14:73–79.
- Puelles, L. and Rubenstein, J.L. (1993) Expression patterns of homeobox and other putative regulatory genes in the embryonic mouse forebrain suggest a neuromeric organization. *Trends Neurosci* 16:472–479.
- Saito, T. and Nakatsuji, N. (2001) Efficient gene transfer into the embryonic mouse brain using in vivo electroporation. *Dev Biol* 240:237–246.
- Sakamoto, N., Fukuda, K., Watanuki, K., Sakai, D., Komano, T., Scotting, P.J. and Yasugi, S. (2000) Role for cGATA-5 in transcriptional regulation of the embryonic chicken pepsinogen gene by epithelial-mesenchymal interactions in the developing chicken stomach. *Dev Biol* 223:103–113.
- Serbedzija, G.N., Fraser, S. and Bronner-Fraser, M. (1990) Pathways of trunk neural crest cell migration in the mouse embryo as revealed by vital dye labelling. *Development* 108:605–612.
- Summerton, J. (1999) Morpholino antisense oligomers: the case for an RNase H independent structural type. *Biochim Biophys Acta* 1489:141–158.
- Summerton, S. and Weller, D. (1997) Morpholino antisense oligomers: design, preparation, and properties. *Antisense Nucleic Acid Drug Dev* 7:187–195.
- Swartz, M., Eberhart, J., Mastick, G.S. and Krull, C.E. (2001) Sparking New Frontiers: Using in Vivo Electroporation for Genetic Manipulations. *Dev Biol* 233:13–21.
- Tabata, H. and Nakajima, K. (2001) Efficient in utero gene transfer system to the developing mouse brain using electroporation: visualization of neuronal migration in the developing cortex. *Neuroscience* 103:865–872.
- Takahashi, M. and Osumi, N. (2002) *Pax6* regulates specification of ventral neurone subtypes in the hindbrain by establishing progenitor domains. *Development* 129:1327–1338.
- Timmer, J., Johnson, J. and Niswander, L. (2001) The use of in ovo electroporation for the rapid analysis of neural-specific murine enhancers. *Genesis* 29:123–132.
- Tomioka, N., Osumi, N., Sato, Y., Inoue, T., Nakamura, S., Fujisawa, H. and Hirata, T. (2000) Neocortical origin and tangential migration of guidepost neurons in the lateral olfactory tract. *J Neurosci* 20:5802–5812.
- Tucker, R.P. (2001) Abnormal neural crest cell migration after the in vivo knockdown of tenascin-C expression with morpholino antisense oligonucleotides. *Dev Dyn* 222:115–119.
- Turnbull, D.H. (2000) Ultrasound backscatter microscopy of mouse embryos. *Methods Mol Biol* 135:235–243.
- Wichterle, H., Turnbull, D.H., Nery, S., Fishell, G. and Alvarez-Buylla, A. (2001) In utero fate mapping reveals distinct migratory pathways and fates of neurons born in the mammalian basal forebrain. *Development* 128:3759–3771.
- Yamasaki, T., Kawaji, K., Ono, K., Bito, H., Hirano, T., Osumi, N. and Kengaku, M. (2001) *Pax6* regulates granule cell polarization during parallel fiber formation in the developing cerebellum. *Development* 128:3133–3144.
- Yasuda, K., Momose, T. and Takahashi, Y. (2000) Applications of microelectroporation for studies of chick embryogenesis. *Dev Growth Differ* 42:203–206.
- Yasugi, S. and Nakamura, H. (2000) Gene transfer into chicken embryos as an effective system of analysis in developmental biology. *Dev Growth Differ* 42:195–197.

Multipolar Migration: The Third Mode of Radial Neuronal Migration in the Developing Cerebral Cortex

Hidenori Tabata^{1,2} and Kazunori Nakajima^{1,2,3}

¹Department of Anatomy, Keio University School of Medicine, Shinjuku-ku, Tokyo 160-8582, Japan, ²Department of Molecular Neurobiology, Institute of DNA Medicine, Jikei University School of Medicine, Minato-ku, Tokyo 105-8461, Japan, and ³Precursory Research for Embryonic Science and Technology, Japan Science and Technology Corporation, Kawaguchi, Saitama 332-0012, Japan

Two distinct modes of radial neuronal migration, locomotion and somal translocation, have been reported in the developing cerebral cortex. Although these two modes of migration have been well documented, the cortical intermediate zone contains abundant multipolar cells, and they do not resemble the cells migrating by locomotion or somal translocation. Here, we report that these multipolar cells express neuronal markers and extend multiple thin processes in various directions independently of the radial glial fibers. Time-lapse analysis of living slices revealed that the multipolar cells do not have any fixed cell polarity, and that they very dynamically extend and retract multiple processes as their cell bodies slowly move. They do not usually move straight toward the pial surface during their radial migration, but instead frequently change migration direction and rate; sometimes they even remain in almost the same position, especially when they are in the subventricular zone. Occasionally, the multipolar cells jump tangentially during their radial migration. Because the migration modality of these cells clearly differs from locomotion or somal translocation, we refer to their novel type of migration as “multipolar migration.” In view of the high proportion of cells exhibiting multipolar migration, this third mode of radial migration must be an important type of migration in the developing cortex.

Key words: cerebral cortex; neuronal migration; radial glial fiber; multipolar cell; mouse; intermediate zone

Introduction

In the developing cerebral cortex, projection neurons are primarily generated in the ventricular zone (VZ) and then move to the developing cortical plate (CP) by means of “radial migration” (Angevine and Sidman, 1961; Berry and Rogers, 1965; Rakic, 1972). Most GABAergic interneurons, however, originate in ganglionic eminences in mice and enter the developing CP via “tangential migration” (Marin and Rubenstein, 2001). Two distinct modes of radial migration, locomotion and somal translocation, have been reported previously (Nadarajah et al., 2001). Locomotion is characterized by cell migration along a radial fiber of a radial glial cell (Rakic, 1972), the fibers of which traverse the entire thickness of the developing cerebral wall. Neurons migrating in this mode have bipolar cell morphology, with a thick leading process and a thin trailing process, and the entire cell moves along the radial fiber. In somal translocation, as the soma of a cell with a long radially directed leading process that terminates at the pial surface advances toward the pial surface, its leading process becomes progressively shorter, whereas its terminal remains at-

tached to the pial surface (Miyata et al., 2001; Nadarajah et al., 2001; Tamamaki et al., 2001).

In contrast to the bipolar or monopolar morphology of the cells that migrate by locomotion or somal translocation, histological analyses of fixed sections of developing cerebral hemisphere using Golgi staining, electron microscopy, or virus vectors expressing green fluorescent protein (GFP) have demonstrated the presence of multipolar cells in the intermediate zone (IZ) (Stensaas, 1967; Shoukimas and Hinds, 1978; Nowakowski and Rakic, 1979; Gadisseux et al., 1990; Noctor et al., 2001; Tamamaki et al., 2001). The radially oriented bipolar or monopolar morphology of locomotion or somal-translocation cells cannot account for the presence of the large proportion of multipolar cells in the IZ, and yet the behavior of these multipolar cells, including whether they indeed migrate, is unknown, because all of the previous analyses have been performed on fixed sections.

We recently established an *in utero* gene transfer system for use in mouse brains that allows plasmid vectors to be introduced into the embryonic cerebral VZ (Tabata and Nakajima, 2001, 2002). We used this system to label migrating cells in the developing cortex with GFP or red fluorescent protein (DsRed) and performed time-lapse observations. Here, we report that multipolar cells express neuronal markers and migrate by a novel mode of radial migration that we refer to as “multipolar migration.” Because the majority of the cells in the IZ–subventricular zone (SVZ) are multipolar, this mode of migration must be an important type of migration in the developing cortex.

Received Aug. 7, 2003; revised Sept. 10, 2003; accepted Sept. 13, 2003.

This work was supported by the Japan Science and Technology Corporation, the Ministry of Education, Culture, Sports, Science and Technology of Japan, the Japan Society for the Promotion of Science, a Keio University Special grant-in-aid for innovative collaborative research projects, and the Sumitomo Foundation. We thank S. Nagata for the EF1 α promoter, J. Miyazaki for the CAG promoter, and R. Hevner for anti-Tbr1.

Correspondence should be addressed to Dr. Kazunori Nakajima, Department of Anatomy, Keio University School of Medicine, 35 Shinanomachi, Shinjuku-ku, Tokyo 160-8582, Japan. E-mail: kazunori@sc.itc.keio.ac.jp.

Copyright © 2003 Society for Neuroscience 0270-6474/03/239996-06\$15.00/0

Materials and Methods

In utero electroporation. All animal experiments were performed according to the guidelines of the Japan Neuroscience Society. Pregnant ICR mice (Japan SLC, Shizuoka, Japan) were deeply anesthetized, and their intrauterine embryos were surgically manipulated as described previously (Nakajima et al., 1997). The enhanced green fluorescent protein (EGFP; Clontech, Cambridge, UK) expression vector with a human elongation factor 1 α (EF1 α) promoter (Uetsuki et al., 1989) or with modified chicken β -actin promoter with cytomegalovirus-immediate early enhancer (CAG) promoter (Niwa et al., 1991) was directly introduced into the VZ by *in utero* electroporation as reported previously (Tabata and Nakajima, 2001). For simplicity, when brains were transfected, for example, with GFP expression vector and EF1 α promoter on embryonic day 13 (E13) and killed on E16, it is indicated as “EF1 α -GFP/E13:E16” in this paper. Red fluorescent protein (DsRed2 or DsRed-Express; Clontech) expression vectors were used for time-lapse analysis.

Time-lapse imaging. Coronal brain slices (200 μ m thick) from the anterior one-third of the cortex were placed on a Millicell-CM (pore size, 0.4 μ m; Millipore, Bedford, MA), mounted in collagen gel, and cultured in Neurobasal medium containing B27 (Invitrogen, San Diego, CA). The dishes were then mounted in a CO₂ incubator chamber (5% CO₂ at 37°C) fitted onto a confocal microscope [LSM510 (Zeiss, Oberkochen, Germany) or FV300 (Olympus Optical, Tokyo, Japan)]. The dorsomedial or lateral region of the cortex was analyzed, and essentially the same results were obtained in both regions. Approximately 10–20 optical Z sections were obtained automatically every 30 min, and ~20 focal planes (~50 μ m thickness) were merged to visualize the shape of the entire cell.

Immunostaining. Tissue samples were prepared as described previously (Tabata and Nakajima, 2001). To detect GABA, the animals were perfused with 4% paraformaldehyde with 0.1% glutaraldehyde. In other cases, 4% paraformaldehyde without glutaraldehyde was used. The primary antibodies used in this study were anti-Hu (1:200; Molecular Probes, Eugene, OR), which recognizes HuC and HuD, anti-calbindin (1:1000; Swant, Bellinzona, Switzerland), anti-GABA (1:500; Sigma, St. Louis, MO), anti-*nestin* (Rat 401; 1:1000; BD Biosciences, San Jose, CA), anti-neurofilament M (1:200; Chemicon, Temecula, CA), anti- β III-tubulin (TuJ1; 1:1000; Babco, Richmond, CA) and anti-Tbr1 (1:1000) (Hevner et al., 2001). The dorsomedial region in the anterior one-third of the cortex was analyzed. Images were acquired with confocal microscopes [LSM410 or LSM510 (Zeiss) or FV300 (Olympus Optical)].

Results

Abundant multipolar neurons are present in the intermediate and subventricular zones

To examine the morphology of migrating neurons, we directly introduced the GFP or DsRed expression vectors into the cells of the cortical VZ *in utero* by electroporation (Tabata and Nakajima, 2001). In the EF1 α -EGFP/E14:E17 brains (see Materials and Methods for the abbreviation), GFP-positive migrating cells were found in the developing CP, IZ, and SVZ (Fig. 1*A,B*). The GFP-expressing cells in the CP in both the dorsomedial cortex (Fig. 1*A*) and the lateral cortex (Fig. 1*B*) assumed a radially oriented bipolar shape with a thick leading process extending toward the pial surface and a thin trailing process, representing the typical locomotion–cell morphology (Fig. 1*C*). In contrast, many of the GFP-positive cells within the IZ–SVZ of both the dorsomedial and lateral cortices exhibited multipolar morphology (Fig. 1*D*), and the multipolar cells were especially abundant in the lower IZ and SVZ. The strong Hu immunoreactivity in the cytoplasm of the multipolar cells (Fig. 1*D*), as well as the positive staining with TuJ1 (Fig. 1*E–G*), indicated that the cells were indeed neurons. To investigate the relationship between the multipolar cells and the radial fibers, we subsequently stained the radial fibers with an anti-*nestin* antibody (Fig. 1*H*). Although some of the thin processes of the multipolar cells were apposed to the radial fibers (Fig. 1*H*, arrowhead), most of them extended independently

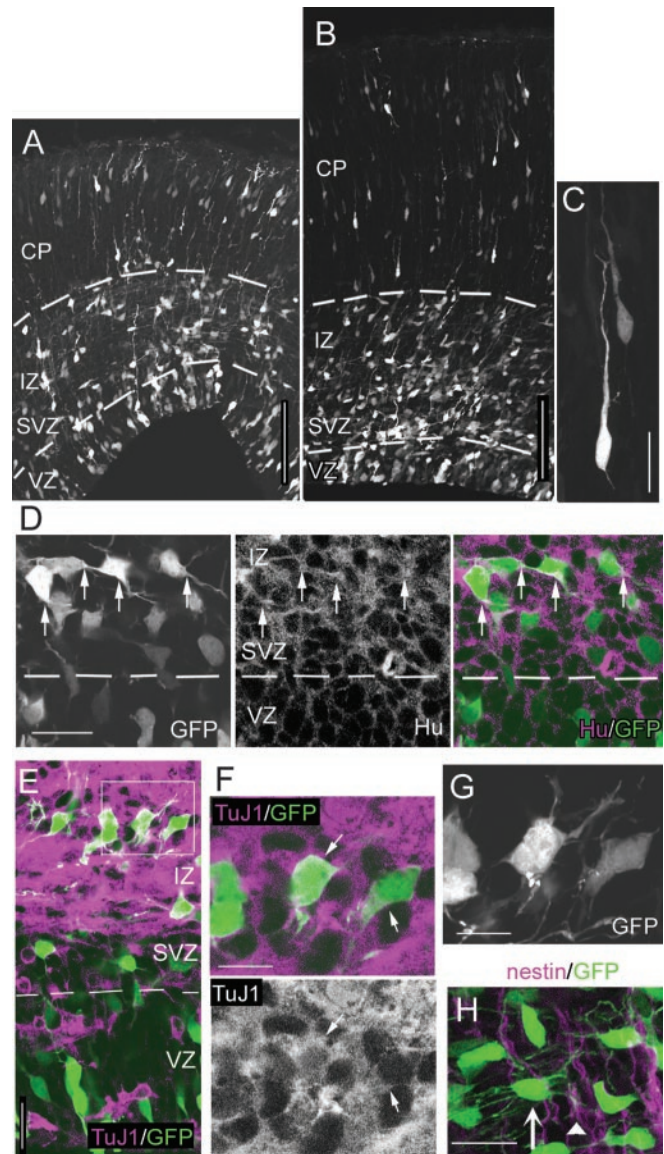


Figure 1. Histological features of multipolar cells in mouse developing cerebral cortex. *A, B*, Coronal sections of brains transfected with EF1 α -GFP/E13:E16. In both the dorsomedial cortex (*A*) and the lateral cortex (*B*), most of the GFP-expressing cells in the IZ and SVZ exhibited multipolar cell morphology, whereas cells in the CP they had a radially oriented bipolar cell morphology. The dashed lines indicate the border between VZ and SVZ, or IZ and CP. *C*, High-magnification views of the GFP-positive cells in the CP. *D–G*, In the CAG-GFP/E14.5:E16 brains, the GFP-positive cells exhibiting multipolar cell morphology in the IZ–SVZ (*D*, left panel; *E, F*; extended focus view of the confocal image in *F* is shown in *G*) expressed the neuron markers Hu (*D*, middle and right panels) and TuJ1 (*E, F*). The dashed line in *D* and *E* indicates the border between VZ and SVZ. The arrows in *D* and *E* indicate the cytoplasm of multipolar cells. *H*, Although some of the thin processes of the multipolar cells were apposed to the radial fibers (arrowhead), which were stained with anti-*nestin*, most of them extended independently from the radial fibers. EF1 α -GFP/E13:E16 brains were analyzed. Scale bars: *A, B*, 100 μ m; *C–E, H*, 20 μ m; *F, G*, 10 μ m.

from the radial fibers, suggesting that the multipolar cells are not associated highly with the radial fibers, unlike locomotion cells.

Multipolar neurons express a marker of projection neurons but not of interneurons

To determine whether the GFP-labeled multipolar neurons were derived from the cortical VZ instead of the ganglionic eminences, we then introduced the vectors into the dorsomedial region of the

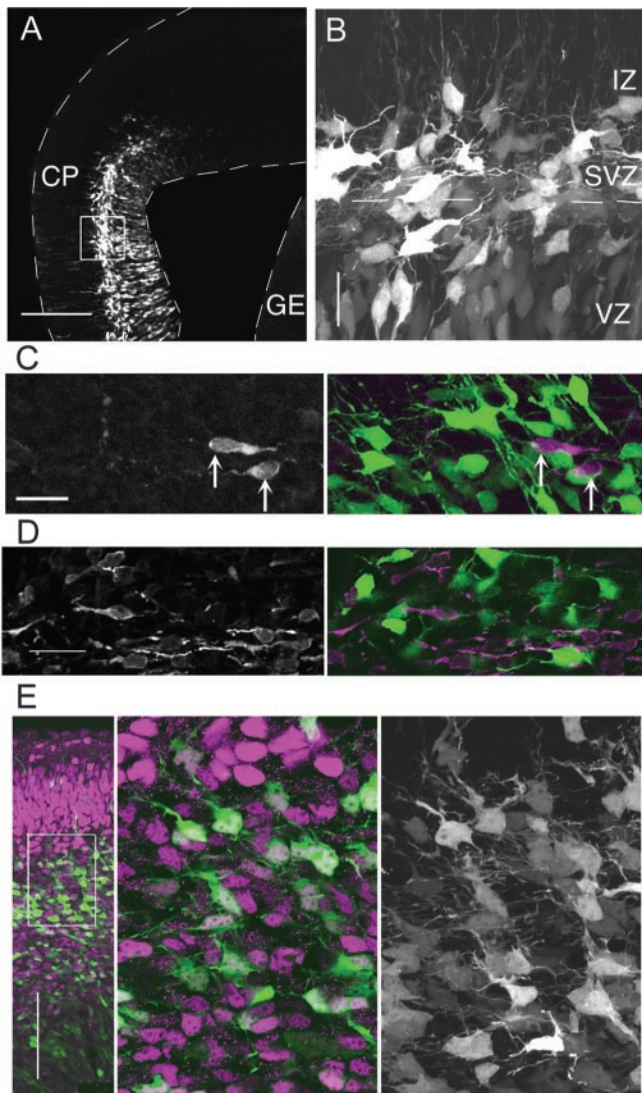


Figure 2. The GFP-labeled multipolar cells originated from the cortical VZ. *A*, Plasmid DNA was injected into the lateral ventricle on one side, and an anode was placed on the opposite side of the injected hemisphere so that the dorsomedial region was labeled selectively (CAG-GFP/E14.5:E16). The dashed lines indicate the margin of the tissue. GE, Ganglionic eminence. *B*, High magnification of the boxed region in *A* revealed that many of the GFP-expressing cells in the IZ–SVZ exhibited multipolar cell morphology, whereas the progenitor cells in the GE were not labeled (*A*). The dashed line indicates the border of VZ and SVZ. *C, D*, The GFP-positive multipolar cells (*C* and *D*, green in the right panels) were calbindin negative (*C*, left panel and purple in the right panel) and GABA negative (*D*, left panel and purple in the right panel). The calbindin-positive cells are indicated by the arrows. The EF1 α -GFP/E13:E16 brains (*C*) and CAG-GFP/E14.5:E16 brains (*D*) were analyzed. *E*, Tbr1 immunostaining on the CAG-GFP/E12.5:E13.5 brains. High expression of Tbr1 was seen in the CP, and low expression was detected in the IZ (purple in the left and middle panels). A single confocal section of the boxed region in the left panel is shown in the middle panel. The GFP-positive (green) cells were Tbr1 positive (purple). The extended-focus view of the green channel of the middle panel revealed that the GFP-positive cells exhibited a multipolar cell morphology (right panel). Scale bars: *A, E*, 200 μ m; *B*, 100 μ m; *C, D*, 20 μ m.

cortical VZ specifically and not into the ganglionic eminences by positioning the cathode ventrolaterally (Fig. 2*A*). Even in these experiments, however, abundant multipolar cells were still observed within the cortical IZ–SVZ (Fig. 2*B*). Moreover, the GFP-positive multipolar cells did not stain positive for calbindin ($n = 0$ of 96) (Fig. 2*C*) or GABA ($n = 0$ of 103) (Fig. 2*D*), two markers expressed by tangentially migrating neurons originating in ganglionic eminences (Anderson et al., 1997). Finally, the GFP-

positive multipolar cells in the IZ–SVZ of the CAG-E12.5:E13.5 brains expressed Tbr1, a marker for subplate (SP) and early generated cortical projection neurons derived from the cortical VZ (Fig. 2*E*) (Hevner et al., 2001). These results suggest strongly that the GFP-positive multipolar cells we investigated in this study were derived from the cortical VZ. However, we have not ruled out the possibility that the tangentially migrating cells derived from the ganglionic eminences may also assume multipolar morphology in the cortical IZ–SVZ, because those cells were not visualized in this study.

Behavior of multipolar neurons

Because the morphology of multipolar cells is very different from cells that migrate by the modes reported previously (locomotion and somal translocation), we attempted to determine whether the multipolar cells were indeed migrating by transfecting mouse brains with a DsRed expression vector *in utero* on E12.5 and performing time-lapse observations of the dorsomedial cortex in slice cultures on E14 (EF1 α -DsRed/E12.5:E14). Many multipolar cells were found in the IZ at this stage of development, and in contrast to locomotion or somal-translocation cells, they did not exhibit fixed cell polarity and were extending and retracting thin processes in various directions in a very dynamic manner (Fig. 3*A, B*) (movie files, available at www.jneurosci.org). Many of the multipolar cells advanced slowly toward the pial surface (Fig. 3*A*, arrow in *B*); however, some of them remained in almost the same position while dynamically moving their processes (Fig. 3*B*, arrowhead). In the examples shown in Figure 3, *A* and *B*, the multipolar cells migrated radially at a rate of 2.3 μ m/hr (Fig. 3*A*) or 1.8 μ m/hr (Fig. 3*B*, arrow). The behavior of the multipolar cells in the lateral cortex was basically similar to their behavior in the dorsomedial cortex (data not shown). However, in CAG-DsRedExpress/E14.5:E18 brains, we observed that many of the migrating cells in the CP had radially oriented bipolar morphology (Fig. 3*C*, cells a–c) (movie file, available at www.jneurosci.org), and these cells migrated toward the pial surface linearly by locomotion. The migration rate of locomotion cells (9–12 μ m/hr) was faster than that of multipolar migration cells (the migration rates of cells a–c were 12.0, 9.6, and 12.0 μ m/hr, respectively). In the upper IZ or the SP, multipolar cells extended major leading processes radially toward the pial surface (Fig. 3*D*). These cells may have been in the process of transforming into the locomotion cells. Because the movement of multipolar cells resembled neither locomotion nor somal translocation, we dubbed this novel type of migration multipolar migration.

To determine further the migration profile of the multipolar cells, we plotted the movements of each multipolar neuron in slice culture (Fig. 4*A*). These experiments revealed that the multipolar cells moved in various directions and changed direction frequently, although they generally tended to move toward the pial surface ultimately. In addition, their migration rates differed from cell to cell and changed over time. Many of the cells occasionally remained in nearly the same position for several hours during their migration (Fig. 4*A*, dotted circles). Thus, whereas the mean migration rate of these multipolar cells was 4.4 μ m/hr (1.6–6.4 μ m/hr), the mean net change in positions per hour in the radial direction was 2.2 μ m [–14 (sometimes they migrated backward) to 55 μ m in 10 hr]. These results indicate that the characteristics of multipolar migration are unique and different from those of locomotion or somal translocation.

While observing the behavior of the multipolar cells, we found that they occasionally jumped tangentially (Fig. 4*B*) (movie file, available at www.jneurosci.org). One of the tangentially oriented

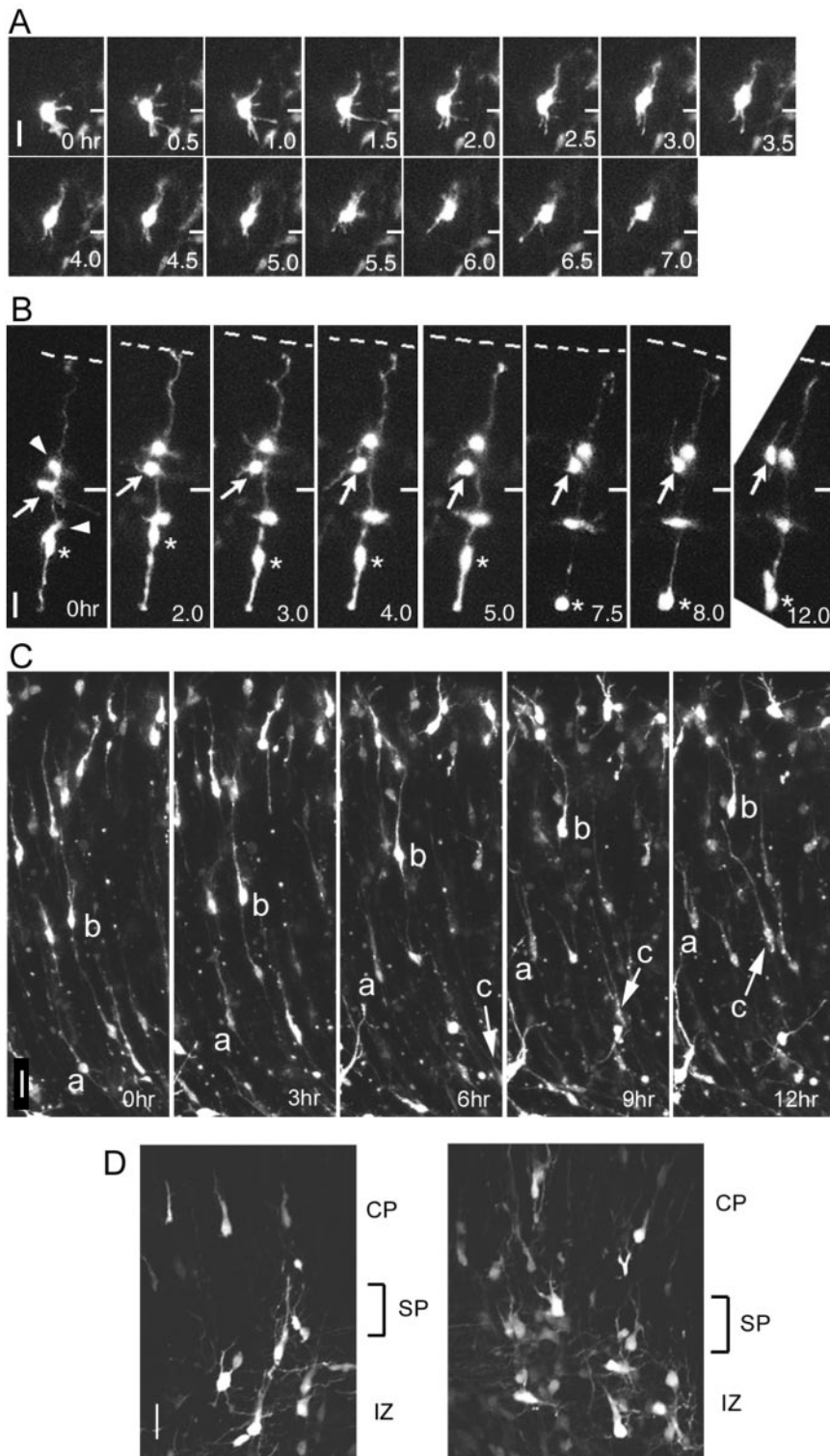


Figure 3. Time-lapse observation of multipolar migration. *A, B*, The movement of the multipolar cells was observed on living slices prepared from EF1 α -GFP/E12.5:E14 brains. *A*, Multipolar cells advanced toward the pial surface (top) very slowly, while extending and retracting multiple processes dynamically. *B*, DsRed-positive multipolar cells were colocalized frequently with DsRed-positive radial glial cells. In this specimen, three labeled multipolar cells (arrowheads and arrow) were colocalized closely with a labeled radial glial cell, the body of which (asterisk) was undergoing mitosis (M phase at $t = 7.5$ hr). One of the multipolar cells, indicated by the arrow, advanced toward the pial surface (dashed line) by means of the dynamic movement of its processes and passed another multipolar cell. The short horizontal bars on the right in *A* and *B* represent the initial position ($t = 0$ hr) of the cell observed. *C*, The locomotion cells within the CP were observed on the living slices taken from the CAG-GFP/E14.5:E18 brains. The migration rates of cells *a–c* were measured (see Results) (movie files, available at www.jneurosci.org). The position of cell *c* is indicated by the arrow. *D*, The multipolar cells near the border between IZ and CP tend to extend major leading processes toward the pial surface. Scale bars, 20 μ m.

processes of these cells thickened transiently, and their cell bodies then translocated in the direction of the thickened major process. Finally, the cells retracted the tangential process and reassumed a multipolar morphology to continue their radial migration toward the pial surface. Thus, multipolar cells may have some affinity for radial fibers during migration, but the affinity did not appear to be very strong.

Because the cell bodies and processes of the multipolar cells tended to be oriented tangentially (mediolateral orientation) when they appeared above the VZ (Figs. 1*A, B*, 2*B*), we hypothesized that the tangential axon bundles in the IZ–SVZ affected multipolar cell orientation and served as the initial target of multipolar migration. To test this hypothesis, we visualized the axons by staining with anti-neurofilament (NF) antibody (Fig. 4*C, D*). The multipolar cells were observed to orient along the axon bundles, suggesting that they might interact with each other (Fig. 4*C*). However, when examined at a later stage, the multipolar cells began to orient tangentially even before they reached the strongly NF-positive structure, suggesting that they may share some unknown directional cues in the lower IZ–SVZ instead (Fig. 4*D*).

To quantitate the population of cells exhibiting multipolar migration, we then counted the multipolar migration cells on the time-lapse sequences in living slices from EF1 α -DsRed/E12.5:E14 brains. Among the 122 cells that were observed to move within the IZ of the dorsomedial cortex, in 107 cells, the mode was multipolar migration (88%). Together, these *in vitro* observations and *in vivo* data from fixed brains indicate that multipolar migration must be used by the major population of migrating cells in the cortical IZ and SVZ.

Discussion
Multipolar migration is a mode of migration distinct from locomotion or somal translocation

We found that the major mode of migration in the IZ–SVZ was multipolar migration, a mode of migration that is distinct from locomotion and somal translocation. The mean net change in positions per hour of the multipolar migration cells (2.2 μ m/hr) was much smaller than that of the locomotion cells in the CP (9–12 μ m/hr). A previous study involving sequential labeling experiments *in vivo* with [3 H]thymidine and bromodeoxyuridine showed that mean net change in positions per hour of migrating neurons in the lower IZ–SVZ of

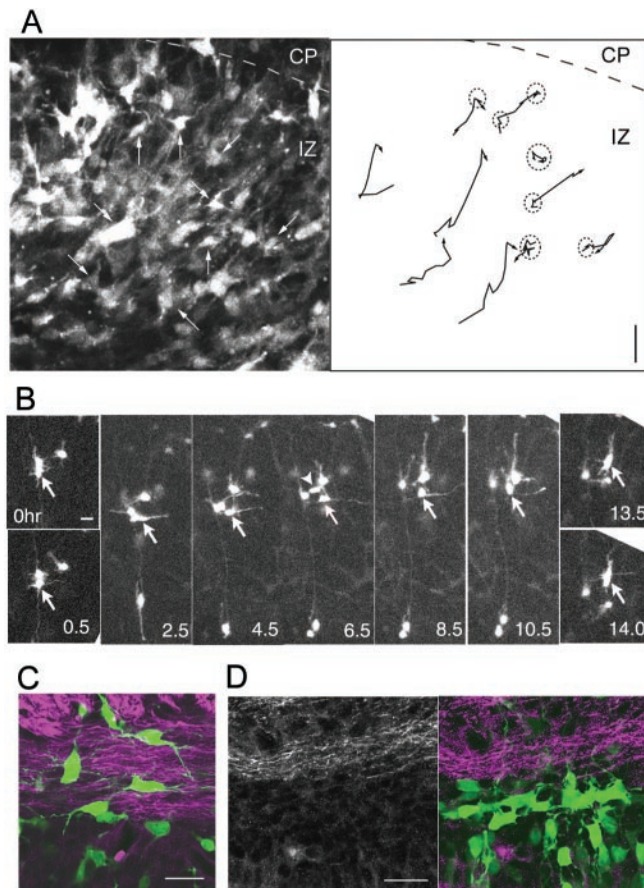


Figure 4. Migratory course of the multipolar neurons. *A*, Tracing of multipolar cell movement. The slices were prepared from CAG-GFP/E12.5:E14 brains, and time-lapse observations were made in the IZ. The position of 10 individual multipolar cells was plotted at 1 hr intervals for 10 hr. The image taken 2 hr after the first time point is shown in the left panel, and the trajectory is shown in the right panel. Many of the multipolar cells occasionally remained in nearly the same positions for several hours during their migration (dotted circles). The border between the IZ and CP is indicated by a dashed line. The traced cells are indicated by the arrows. *B*, Tangential jump of multipolar cells. One multipolar cell (arrow) temporarily assumed locomotion cell-like morphology by extending a thick process tangentially and jumping in that direction ($t = 2.5\text{--}8.5$ hr). The cell then retracted the thick tangential process and extended a radially oriented thick process. Finally, the cell resumed radial multipolar migration toward the pial surface (top) ($t = 10.5\text{--}14$ hr). The other cell (arrowhead; $t = 6.5$) also jumped tangentially ($t = 4.5\text{--}8.5$ hr) (movie file, available at www.jneurosci.org). *C*, *D*, The cell bodies and tangential processes of the multipolar cells (green) tended to be oriented in parallel with the NF-positive axon bundles (purple). CAG-GFP/E14.5:E16 (*C*) or CAG-GFP/E16:E17.5 (*D*) brains were analyzed. Scale bars, 20 μm .

E14.5 mouse embryos was 2 $\mu\text{m}/\text{hr}$ (Takahashi et al., 1996), a finding that is consistent with our observation of multipolar migration cells. The migration rate by locomotion that we observed in this study (9–12 $\mu\text{m}/\text{hr}$) was comparable with that observed by O'Rourke et al. (1992) (11 $\mu\text{m}/\text{hr}$) but slower than reported by Nadarajah et al. (2001) (35 $\mu\text{m}/\text{hr}$). This discrepancy may be attributable to the difference in experimental conditions in the slice culture. Takahashi et al. (1996) reported an *in vivo* migration rate of E14-born cells in the CP of 6.4 $\mu\text{m}/\text{hr}$. Because most migrating cells in the CP seemed to migrate by locomotion (Figs. 1*A–C*, 2*B*), our estimate (9–12 $\mu\text{m}/\text{hr}$) in our slice culture system may be closer to, but still faster than, the *in vivo* migration rate. This may reflect the difference between the *in vivo* and the *in vitro* environment of the migrating neurons.

The three modes of migration may differ in their dependency on the guidance cues for radial migration. In locomotion, the

radial fibers provide the direction of migration and act as the scaffold. If the leading process extending toward the pial surface were maintained, the locomotion cells might be able to migrate along the radial fibers without any additional positional cues. In somal translocation, the ascending process from the cell body reaches the final destination so that migrating neurons can arrive at the final destination without any additional positional cues. In contrast, in multipolar migration, neurons do not associate closely with the radial fibers, and they sometimes jump tangentially during their radial migration. Therefore, it is likely that the multipolar cells sense some directional cue when they resume radial migration. These findings suggest that some environmental factor that directs migrating neurons toward the pial surface exists in the developing cortex.

Biological meaning of multipolar migration

During multipolar migration, multipolar cells repeatedly extend and retract their processes in a very dynamic manner. This kind of behavior is also observed during the pathfinding activity of axonal growth cones while in the “decision region,” in which the growing axon changes direction (Godement et al., 1990; Halloran and Kalil, 1994). These observations suggest that multipolar movement may be needed to search for environmental cues related to the direction of axon growth or radial migration.

Although locomotion cells and somal translocation cells are restricted in their tangential dispersion because of their dependence on radial fibers (locomotion) and long radial processes (somal translocation), multipolar cells seem to be free to migrate in tangential directions (Fig. 4*A,B*). This flexibility may contribute to passing through the IZ when several potential obstacles to radial migration exist, such as afferent and efferent fibers, tangentially migrating neurons, and previous radially migrating neurons.

Although we observed that the multipolar cells accounted for the major population of the GFP-labeled migrating cells in the IZ–SVZ, we did not find multipolar migration cells in the CP, in which most migrating cells exhibited locomotion morphology (Figs. 1*A–C*, 3*C*). These locomotion cells in the CP may have migrated by locomotion all the way from the cortical VZ, and they may be a population independent from the multipolar cells in the IZ–SVZ. Another possibility is that the locomotion CP cells may have derived from multipolar IZ–SVZ cells. If the latter is true, the multipolar cells must have transformed into locomoting cells before entering the CP. When we investigated the morphology of the migrating cells in the IZ–SVZ, we found only a small population of cells exhibiting locomotion (Fig. 1*A,B*). In addition, the multipolar cells generally ultimately migrated toward the pial surface (Fig. 4*A*), expressed neuronal markers (Figs. 1*D–G*, 2*E*), and exhibited locomotion cell-like morphology beneath the CP *in vivo* (Fig. 3*D*); in addition, at least most of them were not apoptotic, as revealed by terminal deoxynucleotidyl transferase-mediated biotinylated UTP nick end labeling staining ($n = 0$ of 107; data not shown) (Thomaidou et al., 1997). These results suggest that the multipolar cells are likely to enter the CP as locomotion cells. Additional experiments, however, will be required to draw a final conclusion.

References

- Anderson SA, Eisenstat DD, Shi L, Rubenstein JLR (1997) Interneuron migration from basal forebrain to neocortex: dependence on Dix genes. *Science* 278:474–476.
- Angevine JB, Sidman RL (1961) Autoradiographic study of cell migration during histogenesis of cerebral cortex in the mouse. *Nature* 192:766–768.

- Berry M, Rogers AW (1965) The migration of neuroblasts in the developing cerebral cortex. *J Anat* 99:691–709.
- Gadisieux JF, Kadhim HJ, van den Bosch de Aguilar P, Caviness VS, Evrard P (1990) Neuron migration within the radial glial fiber system of the developing murine cerebrum: an electron microscopic autoradiographic analysis. *Brain Res Dev Brain Res* 52:39–56.
- Godement P, Salaun J, Mason CA (1990) Retinal axon pathfinding in the optic chiasm: divergence of crossed and uncrossed fibers. *Neuron* 5:173–186.
- Halloran MC, Kalil K (1994) Dynamic behaviors of growth cones extending in the corpus callosum of living cortical brain slices observed with video microscopy. *J Neurosci* 14:2161–2177.
- Hevner RF, Shi L, Justice N, Hsueh Y, Sheng M, Smiga S, Bulfone A, Goffinet AM, Campagnoni AT, Rubenstein JL (2001) *Tbr1* regulates differentiation of the preplate and layer 6. *Neuron* 29:353–366.
- Marin O, Rubenstein JL (2001) A long, remarkable journey: tangential migration in the telencephalon. *Nat Rev Neurosci* 2:780–790.
- Miyata T, Kawaguchi A, Okano H, Ogawa M (2001) Asymmetric inheritance of radial glial fibers by cortical neurons. *Neuron* 31:727–741.
- Nadarajah B, Brunstrom JE, Grutzendler J, Wong RO, Pearlman AL (2001) Two modes of radial migration in early development of the cerebral cortex. *Nat Neurosci* 4:143–150.
- Nakajima K, Mikoshiba K, Miyata T, Kudo C, Ogawa M (1997) Disruption of hippocampal development *in vivo* by CR-50 mAb against reelin. *Proc Natl Acad Sci USA* 94:8196–8201.
- Niwa H, Yamamura K, Miyazaki J (1991) Efficient selection for high-expression transfectants with a novel eukaryotic vector. *Gene* 108:193–199.
- Noctor SC, Flint AC, Weissman TA, Dammerman RS, Kriegstein AR (2001) Neurons derived from radial glial cells establish radial units in neocortex. *Nature* 409:714–720.
- Nowakowski RS, Rakic P (1979) The mode of migration of neurons to the hippocampus: a Golgi and electron microscopic analysis in foetal rhesus monkey. *J Neurocytol* 8:697–718.
- O'Rourke NA, Dailey ME, Smith SJ, McConnell SK (1992) Diverse migratory pathways in the developing cerebral cortex. *Science* 258:299–302.
- Rakic P (1972) Mode of cell migration to the superficial layers of fetal monkey neocortex. *J Comp Neurol* 145:61–84.
- Shoukimas GM, Hinds JW (1978) The development of the cerebral cortex in the embryonic mouse: an electron microscopic serial section analysis. *J Comp Neurol* 179:795–830.
- Stensaas LJ (1967) The development of hippocampal and dorsolateral pallial regions of the cerebral hemisphere in fetal rabbits. II. Twenty millimeter stage, neuroblast morphology. *J Comp Neurol* 129:71–84.
- Tabata H, Nakajima K (2001) Efficient *in utero* gene transfer system to the developing mouse brain using electroporation: visualization of neuronal migration in the developing cortex. *Neuroscience* 103:865–872.
- Tabata H, Nakajima K (2002) Neurons tend to stop migration and differentiate along the cortical internal plexiform zones in the Reelin signal-deficient mice. *J Neurosci Res* 69:723–730.
- Takahashi T, Nowakowski RS, Caviness Jr VS (1996) Interkinetic and migratory behavior of a cohort of neocortical neurons arising in the early embryonic murine cerebral wall. *J Neurosci* 16:5762–5776.
- Tamamaki N, Nakamura K, Okamoto K, Kaneko T (2001) Radial glia is a progenitor of neocortical neurons in the developing cerebral cortex. *Neurosci Res* 41:51–60.
- Thomaidou D, Mione MC, Cavanagh JF, Parnavelas JG (1997) Apoptosis and its relation to the cell cycle in the developing cerebral cortex. *J Neurosci* 17:1075–1085.
- Uetsuki T, Naito A, Nagata S, Kaziro Y (1989) Isolation and characterization of the human chromosomal gene for polypeptide chain elongation factor-1 alpha. *J Biol Chem* 264:5791–5798.

Radial Migration of Superficial Layer Cortical Neurons Controlled by Novel Ig Cell Adhesion Molecule MDGA1

Akihide Takeuchi and Dennis D. M. O'Leary

Molecular Neurobiology Laboratory, The Salk Institute, La Jolla, California 92037

MAM (meprin/A5 protein/receptor protein tyrosine phosphatase mu) domain glycosylphosphatidylinositol anchor 1 (MDGA1), a unique cell surface glycoprotein, is similar to Ig-containing cell adhesion molecules that influence neuronal migration and process outgrowth. We show in postnatal mice that MDGA1 is expressed by layer 2/3 neurons throughout the neocortex. During development, MDGA1 is expressed in patterns consistent with its expression by migrating layer 2/3 neurons, suggesting a role for MDGA1 in controlling their migration and settling in the superficial cortical plate. To test this hypothesis, we performed loss-of-function studies using RNA interference (RNAi) targeting different sequences of mouse MDGA1. RNAi or empty vectors were coelectroporated with an enhanced green fluorescent protein reporter *in utero* into the lateral ventricle at embryonic day 15.5 to transfect progenitors of superficial layer neurons; the distributions of transfected neurons were analyzed late on postnatal day 0. We found a direct correlation between effectiveness of an RNAi in suppressing MDGA1 expression and disrupting migration of superficial layer neurons. An RNAi with no effect on MDGA1 expression has no effect on the migration. In contrast, an RNAi that suppresses MDGA1 expression also blocks proper migration of transfected superficial layer neurons, with essentially all transfected cells found deep in the cortical plate or beneath it. This migration defect is rescued by cotransfection of a rat MDGA1 expression construct along with the effective RNAi, confirming that the RNAi effect is specific to diminishing mouse MDGA1 expression. RNAi transfections of deep layer neurons that do not express MDGA1 do not significantly affect their migration. We conclude that MDGA1 acts cell autonomously to control the migration of MDGA1-expressing superficial layer cortical neurons.

Key words: cell adhesion molecules; cortical development; cortical lamination; Ig superfamily; *in utero* electroporation; RNAi

Introduction

The mammalian neocortex is distinguished from other regions of the cerebral cortex by its six major layers. Each layer is comprised of a heterogeneous population of neurons broadly classified into two general types: glutamatergic, including all projection neurons, and GABAergic interneurons. Most GABAergic interneurons are generated within the medial and caudal ganglionic eminences and migrate tangentially in the intermediate zone (IZ) or marginal zone (MZ) until they reach their cortical destination, whereupon they turn and migrate radially into the cortical plate (CP) (Marin and Rubenstein, 2003; Kriegstein and Noctor, 2004). Glutamatergic neurons are generated by progenitors within the ventricular zone (VZ) and subventricular zone (SVZ) of dorsal telencephalon and migrate radially along processes of radial glia into the overlying CP in an “inside-out” pattern [i.e., early-born neurons form deeper layers and later-born neurons migrate past them to form more superficial layers (Rakic, 1972; Kriegstein and Noctor, 2004)].

Molecules required for radial migration and inside-out cortical lamination include reelin, a protein secreted by Cajal–Retzius neurons of the MZ, its receptors, the very low-density lipoprotein receptor/apolipoprotein E receptor type 2, and downstream components of this signaling pathway that influence migration in part through regulating cytoskeletal proteins, including doublecortin (Bielas et al., 2004; Tsai and Gleason, 2005). The POU domain transcription factors Brn-1 and Brn-2 also have roles in patterning of superficial layers (McEvelly et al., 2002; Sugitani et al., 2002). Cell adhesion molecules (CAMs) play important roles in the interactions of migrating neurons with glial processes (Zheng et al., 1996; Anton et al., 1999). Two CAMs involved in neuronal migration are astrotactin (Adams et al., 2002) and the integrin $\alpha 3 \beta 1$, which to date is the only CAM reported to control cortical radial migration (Anton et al., 1999; Dulabon et al., 2000).

Here, we report a role in cortical radial migration for a unique Ig superfamily protein, meprin/A5 protein/receptor protein tyrosine phosphatase mu (MAM) domain glycosylphosphatidylinositol anchor 1 (MDGA1), that we originally cloned in the rat (Litwack et al., 2004). MDGA1, an IgCAM anchored to the extracellular surface of the cell membrane by a GPI-linkage, contains six Ig domains, a fibronectin III domain, and uniquely for IgCAMs, a MAM domain (Litwack et al., 2004). MDGA1 is structurally similar to other IgCAMs, such as the L1 family and axonin 1, which have roles in cell adhesion, migration, and process out-

Received Nov. 18, 2005; revised Feb. 18, 2006; accepted March 14, 2006.

This work was supported by the National Institutes of Health (D.D.M.O.) and a fellowship from Uehara Memorial Foundation (A.T.). We thank David Litwack for early input and Carlos Garcia for comments. None of the authors has a financial interest related to this work.

Correspondence should be addressed to Dennis D. M. O'Leary, Molecular Neurobiology Laboratory, The Salk Institute, 10010 North Torrey Pines Road, La Jolla, CA 92037. E-mail: doleary@salk.edu.

DOI:10.1523/JNEUROSCI.4935-05.2006

Copyright © 2006 Society for Neuroscience 0270-6474/06/264460-05\$15.00/0

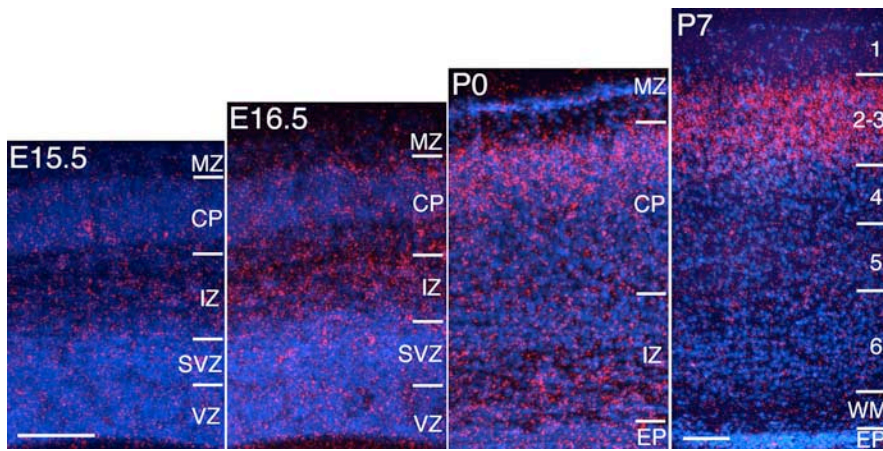


Figure 1. Laminal expression of MDGA1 in the developing cortex. *In situ* hybridization of MDGA1 expression in the developing mouse cortex is shown. At E15.5, MDGA1 is modestly expressed in the IZ. At P0, expression is robust in the CP, and dense clusters of silver grains (red) deeper in the CP and IZ suggest MDGA1 expression by migrating neurons. By P7, robust expression is localized to layers 2/3. EP, Ependymal layer; WM, white matter. Scale bars, 100 μ m; bar in E15.5 is E15.5 to P0.

growth (Walsh and Doherty, 1997; Panicker et al., 2003). We cloned full-length mouse MDGA1 and show that it is expressed in neocortex by layer 2/3 neurons throughout their development. We hypothesize that MDGA1 is involved in controlling the migration and lamination of layer 2/3 neurons. We address this issue using RNA interference (RNAi) combined with *in utero* electroporation in mice, an approach recently used to reveal a function for doublecortin in radial migration of cortical neurons (Bai et al., 2003).

Materials and Methods

Animals. C57BL/6 mice were used to examine MDGA1 expression and to identify its cDNA sequence. Timed pregnant ICR mice were used for *in utero* electroporation. The morning of the vaginal plug is embryonic day 0.5 (E0.5), and the first postnatal day (P) is P0. Experiments were done following institutional guidelines and approved protocols.

Microscopy. Digital images were obtained with a Zeiss (Thornwood, NY) LCM510 confocal microscope or a Retiga digital camera on a Nikon (Tokyo, Japan) Microphot microscope with OpenLab software (Improvision, Coventry, UK).

In situ hybridization. Radioactive *in situ* hybridization of MDGA1 was done on wild-type C57BL/6 mouse embryos and neonates from E9.5 to P7 as described previously (Litwack et al., 2004).

Vectors and in utero electroporation. Four different targeted regions that only match with MDGA1 cDNA sequence were selected to make H1 promoter-based RNAi vectors (pSUPER) (Brummelkamp et al., 2002). The four 19-nucleotide target sequences are as follows: M1, GGAG-GATAACATCAGCGAG; M2, GTCTATCCGCGTGGACGTG; M5, CATTCTCAGAGACAGTA; M6, CGTACGACCCCGGGAGGCT. To evaluate their efficiency, each RNAi vector, or as a control an empty pSUPER ('E1') vector, was cotransfected with a Myc-tagged MDGA1 expressing vector in pcDNA3.1 (–)/Myc-His B (Invitrogen, San Diego, CA) (RNAi, 4.0 μ g; MDGA1-Myc, 1.0 μ g) into COS-7 cells using Polyfect Transfection Reagent (Qiagen, Hilden, Germany). After 24 h, expression of MDGA1-Myc protein was visualized with anti-Myc mouse monoclonal antibody (9E10) and a fluorescent secondary. Quantification of labeling was done using NIH Image and Adobe Photoshop (Adobe Systems, San Jose, CA) as described previously (Pak et al., 2004). To determine relative MDGA1 protein levels, total pixel intensity of fluorescence for each RNAi vector was expressed as a percentage of that obtained with the E1 control vector (normalized as 100%). The number of MDGA1-expressing cells was also counted and indicated as a corrected absolute number. Immunolabeled cells were marked using NIH Image. Counts were done with thresholds set at four different pixel intensity levels (>50, >100, >150, >200; software maximum is 256). Experi-

ments were done five times using the same conditions, normalized between each experiment.

Plasmids used for *in utero* electroporation were prepared using the EndoFree Plasmid kit (Qiagen). To fluorescently label cells transfected *in vivo* with RNAi, we cotransfected a pCAG-enhanced green fluorescent protein (eGFP) vector (Saito and Nakatsuji, 2001). One to 2 μ l of plasmid (molecular ratio for pCAG-GFP and RNAi vectors, 1:3; final concentration of mixed DNA, 1.5 μ g/ μ l) with Fast Green (0.01%; Sigma, St. Louis, MO) in PBS were microinjected using fine-tipped glass capillaries into the right lateral ventricle of each embryo. For the "rescue" experiments, the molecular ratio for the M1 RNAi, pCMV empty vector or pCMV-rMDGA1, and pCAG-GFP is 3:2:1, and the final concentration of mixed DNA is 1.5 μ g/ μ l. Electroporation was done by five pulses at 30 V discharge with a duration of 50 ms at 950 ms intervals. Brains were fixed and coronally sectioned either 24 h later to confirm efficiency and restriction of electroporations or late on P0 for analyses.

Results

A single full-length mouse MDGA1 cDNA was isolated by reverse transcription-PCR from a cDNA library of P7 mouse basilar pons. Homologies in the coding region of cDNA and protein sequences (supplemental Fig. S1, available at www.jneurosci.org as supplemental material) are 94 and 93% between mouse and rat, respectively, and 89 and 92% between mouse and human, respectively.

In situ hybridization reveals a weak transient expression of MDGA1 early in cortical development, from E9.5 to E13.5, limited to the MZ/preplate (data not shown). At E15.5 and later, MDGA1 expression is no longer detected in the MZ (Fig. 1). Signal above background is not detected at any age in the VZ/SVZ. At E16.5, modest expression is evident in the IZ. By P0, a band of MDGA1 expression is clearly evident in the superficial CP (the dense CP that will differentiate into layers 2/3); in addition, scattered cells deeper in the CP and IZ express MDGA1. By P7, expression of MDGA1 is limited to layers 2/3 throughout most of the cortex (Fig. 1) but is not detected in adults (data not shown). Layer 2/3 neurons are generated from E15 through E17, with peak generation on E16 (Takahashi et al., 1999); a substantial proportion reach the superficial CP by birth (Bayer and Altman, 1991). Thus, these data indicate that MDGA1 is expressed by layer 2/3 neurons during their migration and settling in the CP.

To investigate a role for MDGA1 in the migration of superficial layer neurons, we adopted small interference RNA (RNAi) to suppress MDGA1 expression using a pSUPER vector to produce short hairpin RNAs (Brummelkamp et al., 2002) by *in utero* electroporation in mice. Four RNAi vectors were made with unique nucleotide sequences of inter-Ig domains specific to mouse MDGA1 (Fig. 2A). The RNAi vectors vary in their effectiveness in suppressing MDGA1 protein expression, shown by cotransfecting each vector and a myc-tagged MDGA1 expression construct into COS-7 cells (Fig. 2B). Quantitation of relative levels of MDGA1 protein or number of MDGA1-expressing cells revealed by fluorescence immunostaining for the myc-tag shows that the M1 RNAi vector is very effective in suppressing MDGA1 expression, whereas the M6 RNAi vector has no detectable effect and is indistinguishable from the empty pSUPER ('E1') vector (Fig. 2C,D).

For our *in vivo* studies, we used the M1 RNAi vector to suppress MDGA1 expression, and both the E1 empty vector and the M6 RNAi vector as controls for potential nonspecific effects of RNAi and vector expression. We performed *in utero* electroporations of the vectors in E15.5 embryos; an eGFP vector was coelectroporated to mark cells transfected with the RNAi or E1 vectors (Fig. 3A). Because of the timing of these transfections and the dynamics of transgene expression, the majority of the GFP-marked cells should be layer 2/3 neurons, although a very small proportion of layer 4 neurons are generated after E15.5 and therefore could be transfected (Takahashi et al., 1999). Embryos examined 1 d later show discrete transfection domains of GFP-labeled cells within the VZ and SVZ and restricted to dorsal telencephalon (data not shown). To determine the effect of the transfections on neuronal migration, electroporated mice were perfused late on P0, when a substantial proportion of layer 2/3 neurons have reached the superficial CP; only healthy appearing nursing pups were fixed. Twenty-three of the 26 control transfected brains (coelectroporated with GFP, and either M6 RNAi or E1 vectors) and 31 of the 33 M1/GFP cotransfected brains had cortical GFP signal visible in whole mounts fixed at P0.

Brains with similar transfection domains were sectioned: these included 10 control transfected brains (five each of M6 and E1 vectors) and 12 M1 transfected brains. No morphological defects are evident in these transfected brains, and cortical architecture appears normal in 4',6'-diamidino-2-phenylindole (DAPI)-stained sections. Essentially all of the GFP-labeled cells have a pyramidal-like morphology characteristic of layer 2/3 neurons and immunostain for the neuronal marker TuJ1 (class III β -tubulin) (supplemental Fig. S2, available at www.jneurosci.org as supplemental material); however, their laminar distribution differs substantially between brains electroporated with the control vectors (M6 RNAi or E1 empty) versus the M1 RNAi vector. In brains transfected with either the E1 (Fig. 3A) or M6 vector (Fig. 3B), the majority of GFP-labeled cells are in the superficial layers in a distribution that closely resembles the distribution of MDGA1-expressing cells in nontransfected P0 cortex (Fig. 1). In contrast, in brains transfected with the M1 vector, the majority of GFP-labeled cells are deep in the CP or beneath it in the IZ or deeper (Fig. 3C).

The laminar (i.e., radial) distributions of GFP-labeled cells were quantitated at late

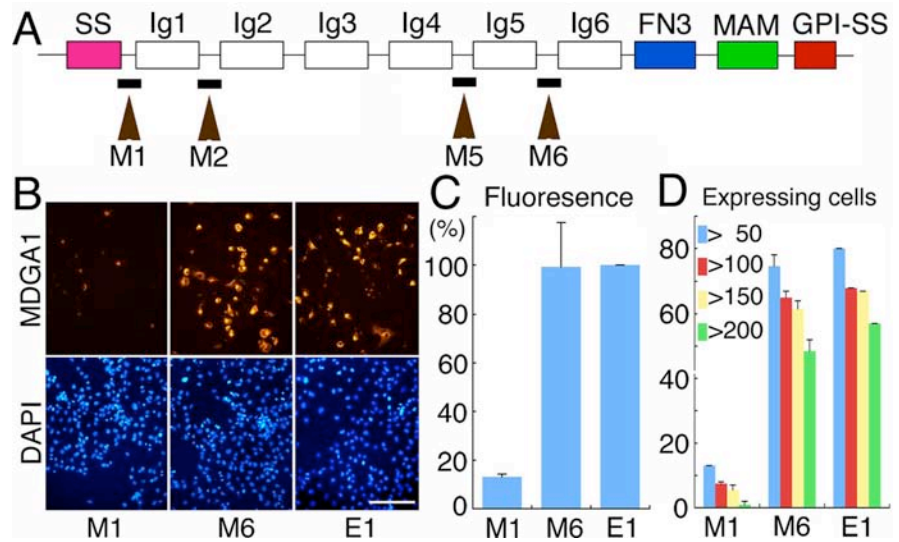


Figure 2. Targeted sequences for RNAi vectors differentially suppress MDGA1 protein expression *in vitro*. *A*, MDGA1 domain structure and selected target regions to make RNAi vectors; the four target regions (M1, M2, M5, M6) were 19 bp sequences located between the Ig domains. SS, Signal peptide sequence; FN3, fibronectin type 3 repeat; MAM, MAM domain; GPI, glycosylphosphatidylinositol anchor. *B*, COS-7 cells cotransfected with a pcDNA3.1 vector containing MDGA1 cDNA tagged with a Myc epitope and an RNAi pSUPER vector or an empty pSUPER vector (E1); RNAi vector name (M1, M6) denotes sequence location shown in *A*. Shown is immunofluorescence using a Myc antibody 24 h after transfection; the secondary antibody was conjugated to Alexa568 (orange). Cultures are DAPI stained (blue). Scale bar, 100 μ m. *C*, Histogram of fluorescence intensity of MDGA1-Myc protein. *D*, Histogram of the number of MDGA1-positive cells with a total pixel intensity above the indicated thresholds. Quantitative data for M2 is statistically indistinguishable from that shown in *C* and *D* for M1 and M5 from that shown for M6.

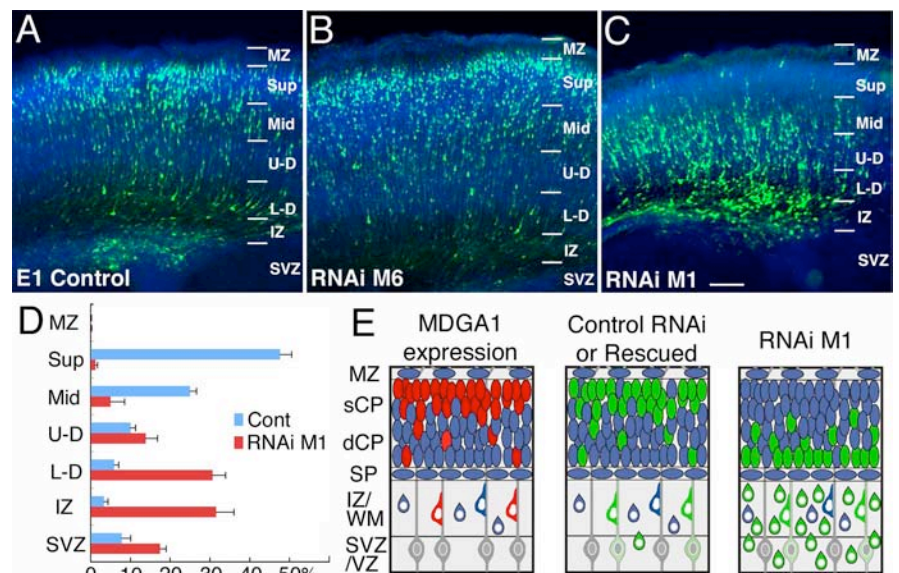


Figure 3. Transfection of M1 RNAi to suppress MDGA1 selectively results in aberrant deep distribution of superficial layer neurons. Distribution of GFP-labeled neurons late on P0 following cotransfections on E15.5 with a GFP and E1 vector (*A*), GFP and M6 RNAi vector (*B*), and GFP and M1 RNAi vector (*C*). *D*, Five M1 cases and five control cases (4 E1 and 1 M6) were quantitatively analyzed. The cortical wall was subdivided as indicated, and numbers of GFP-labeled transfected cells in each layer were counted and expressed as a percentage of the total. Statistical analyses comparing the number of labeled cells in each layer between control and M1 transfected cases (ANOVA, Bonferroni's test) are shown. Statistical difference is seen for each set of layers ($p < 0.01$) except MZ and U-D layers. Scale bars, 100 μ m. *E*, Schematics of late P0 cortex showing an expression pattern of MDGA1 and distribution of GFP-labeled neurons transfected with M1 RNAi or control (M6 RNAi, E1) vectors at E15.5. Expression of MDGA1 is similar to distribution of GFP-labeled neurons transfected with control vectors or in rescue experiments (cotransfections with M1 RNAi and rat MDGA1 cDNA vectors). However, distribution of GFP-labeled neurons transfected with an M1 RNAi vector is aberrantly displaced deep. sCP, Superficial cortical plate; dCP, deep cortical plate; Sup, superficial CP; Mid, middle CP; U-D, upper-deep CP; L-D, lower-deep CP; others are as in Figure 1.

P0 from sections of electroporated brains with very similar transfection domains (five brains electroporated with the M1 RNAi vector and five with control vectors: one M6 RNAi and four E1 empty vectors). In the controls, the mean number of GFP-labeled cells is 370 ± 29 (total of 1851; range, 270–448); the M1 cases have a mean of 268 ± 30 labeled cells (total of 1342; range, 196–364).

In control transfected brains, 74% of GFP-labeled cells are in the upper half of the CP, with 49% in the superficial most quarter of the CP (the dense CP that will become layers 2/3) (Fig. 3D). In contrast, in M1 transfected brains, only 6% of GFP-labeled cells are in the upper half of the CP, with virtually no labeled cells (1%) in the superficial most quarter of the CP; 80% of all labeled cells are in the deepest one-quarter of the CP or beneath it (Fig. 3D). The difference in the distribution of GFP-labeled cells between control and M1 transfected brains is statistically significant for each “layer,” with the exception of the MZ, which contains virtually no labeled cells, and the “upper-deep” layer of the CP, which is the layer where the transition occurs in the superficial versus deep bias in the distribution of transfected cells between control and M1 electroporated brains (Fig. 3D). Thus, transfection with the M1 RNAi vector in migrating layer 2/3 neurons inverts their distribution from superficial to deep (Fig. 3D).

As described in Figure 2, the M6 vector has no detectable effect on expression of MDGA1 *in vitro*, whereas the M1 vector substantially suppresses it (Fig. 2). We also analyzed the effect of these RNAi vectors on MDGA1 expression *in vivo* and obtained similar findings; the M6 vector has no detectable effect on MDGA1 expression ($n = 3$) (Fig. 4A,C), whereas MDGA1 expression is diminished in correlation with domains of M1 transfections ($n = 2$) (Fig. 4B,D). Thus, both the *in vitro* and *in vivo* data indicate that the M1 RNAi vector selectively diminishes MDGA1 expression, whereas the M6 RNAi vector does not.

To corroborate further the specificity of the M1 RNAi vector for selectively suppressing MDGA1, resulting in aberrant migration of MDGA1 expressing layer 2/3 neurons, we did two complementary experiments. In the first set, we performed a “rescue” experiment in which we repeated the same M1/GFP transfections at E15.5 but cotransfected with either a rat MDGA1 cDNA expression construct ($n = 2$) or as a control with an empty expression vector ($n = 2$). Importantly, the M1 vector against mouse MDGA1 has only a one nucleotide mismatch with the same sequence stretch in the rat MDGA1 (Fig. 4F). When analyzed late on P0, the distribution of GFP-labeled cells in cases cotransfected with the M1 RNAi and control expression vectors are qualitatively the same as in cases transfected with only the M1 RNAi vector (i.e., the cells exhibit a migration defect and are distributed deep to their normal positions) (Fig. 4E). In contrast, in cases cotransfected with the M1 RNAi and rat MDGA1 expression vectors, a substantial proportion of the GFP marked cells are positioned superficially in the CP (Fig. 4F). Thus, overexpression of rat MDGA1 in cells transfected with the M1 RNAi mostly rescues the migration defect. In the second set of experiments, we show that transfections at E12.5 of the M1 RNAi vector into deep layer neurons that do not express MDGA1 does not disrupt their migration (supplemental Fig. S3, available at www.jneurosci.org as supplemental material). Together, these findings demonstrate the specificity of the M1 RNAi for mouse MDGA1 and indicate that the defective migration of layer 2/3 neurons transfected with M1 RNAi is specific to their diminished expression of MDGA1.

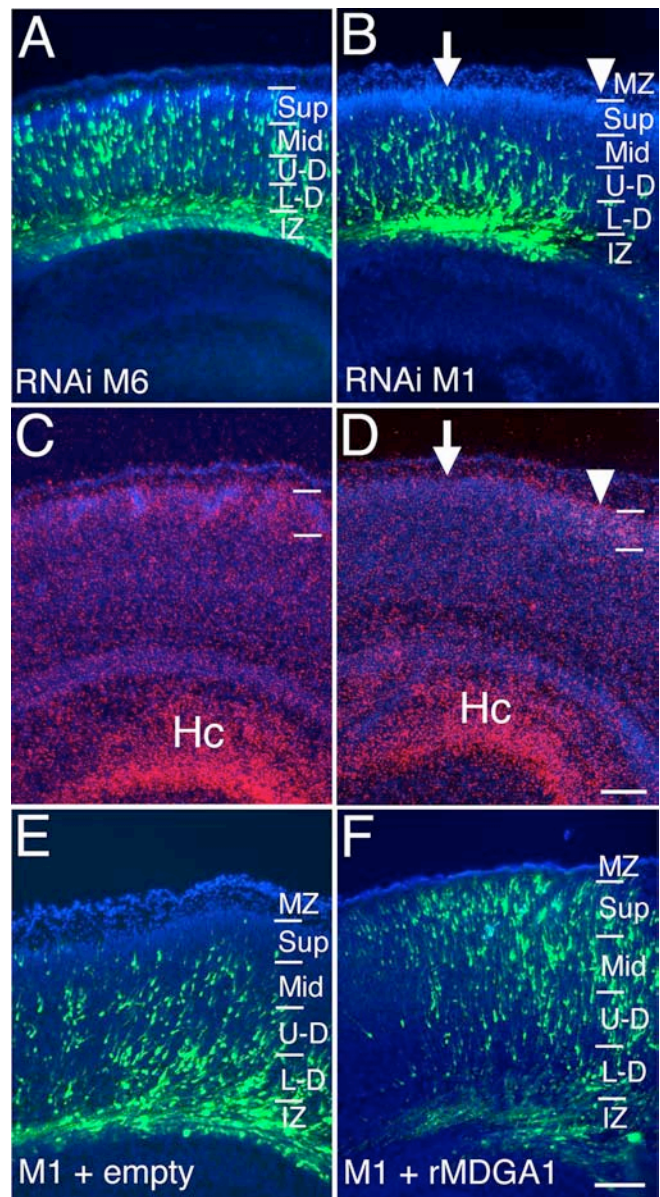


Figure 4. Differential suppression of MDGA1 expression *in vivo* by mouse RNAi vectors with rescue of RNAi-induced migration defect by cotransfection of rat MDGA1. **A–D**, Distribution of GFP-labeled neurons late on P0 following cotransfection with GFP and M6 (**A**) or GFP and M1 RNAi vectors at E15.5 (**B**). *In situ* hybridization using S35-labeled riboprobes for MDGA1 (**C**, **D**) on adjacent sections of **A** and **B**, respectively. M6 RNAi transfection has no detectable effect on MDGA1 expression. However, MDGA1 expression is diminished in superficial layers above the domain of M1 RNAi transfection (arrow) but not adjacent to it (arrowhead). **E**, **F**, Distribution of radially migrating neurons cotransfected with M1 RNAi plus empty pCMV plus GFP vectors (control) (**E**) and M1 RNAi plus pCMV rat-MDGA1 (rMDGA1) plus GFP vectors (**F**). M1 RNAi target sequence (GGAGGATAACATCAGCGAG) and rat MDGA1 cDNA (GGAGGATAAATCAGCGAG) have a one nucleotide mismatch (bolded). In control cases (**E**), most GFP-labeled cells are deep, and virtually none are in the superficial CP. As shown in **F**, cotransfection with rat MDGA1 expression vector essentially corrects the migration defect and shifts distribution of GFP-labeled cells compared with **D**, with many in superficial CP. Scale bars, 100 μm. Hc, Hippocampal formation; other abbreviations are as in Figure 1.

Discussion

We show that MDGA1, a unique IgCAM, is expressed in mouse neocortex by layer 2/3 neurons during their migration and settling superficially in the CP. We go on to show, using RNAi and *in utero* electroporation, that suppression of MDGA1 expression in migrating layer 2/3 neurons disrupts their migration, and over

the period of our analyses prevents the transfected neurons from reaching the superficial CP (Fig. 3E).

To generate the RNAi vectors, we chose stretches of cDNA between the Ig domains, because they have the least homology to other genes. These RNAi vectors have varying effectiveness in suppressing MDGA1 expression. Importantly, we found a direct correlation between the effectiveness of an RNAi vector in suppressing MDGA1 expression, both *in vitro* and *in vivo*, and its ability to disrupt *in vivo* the migration of layer 2/3 neurons: the M1 RNAi vector blocks MDGA1 expression and also blocks proper migration of layer 2/3 neurons, whereas the M6 RNAi vector has no evident effect on MDGA1 expression nor on migration.

These findings argue for the specificity of the effect of the M1 RNAi vector, which we also directly demonstrated by rescuing the M1 RNAi induced migration defect by cotransfecting a rat MDGA1 expression vector with the M1 RNAi vector (Fig. 3E). The mouse MDGA1 sequence against which the M1 RNAi is directed has only a single nucleotide difference from the equivalent sequence of rat MDGA1, which strongly argues for the specificity of the M1 RNAi for mouse MDGA1. Other findings also strongly imply that the observed migration defect is caused by the suppression of MDGA1 in the migrating neurons themselves. First, MDGA1 is expressed by layer 2/3 neurons as they are migrating and forming the superficial layer of the CP but is not expressed by VZ/SVZ cells, and therefore not by radial glia that guide migrating neurons to the CP (Rakic, 1972). In addition, at the developmental stages at which we have performed the *in utero* electroporations, MDGA1 is not expressed by cells in the MZ and therefore not by Cajal–Retzius neurons that express reelin, a protein required for proper radial migration of cortical neurons and CP lamination (D'Arcangelo et al., 1995). Essentially no cells in the MZ are transfected and therefore could not be influenced by the vectors. Additionally, transfections done with the E1 control and M1 RNAi vectors at E12.5, coincident with the generation of deep layer neurons that do not express MDGA1, do not appear to affect the migration of the transfected neurons (supplemental Fig. S3, available at www.jneurosci.org as supplemental material). Therefore, we conclude that the aberrant migration of superficial layer neurons transfected with the M1 RNAi vector is caused by a cell autonomous effect of the suppression of MDGA1 protein.

Our findings indicate a critical role of MDGA1 in the proper migration of superficial layer cortical neurons that normally express it. RNAi suppression of MDGA1 expression results in a failure of superficial layer neurons to reach even the upper half of the CP, and essentially all transfected neurons are very deep in the CP or beneath it (Fig. 3E). This aberrant deep distribution of superficial layer neurons could be attributable to a dramatic slowing in their migration or to a defect in their final laminar distribution. A related issue is whether MDGA1 is required for the formation of layer 2/3. However, these issues are difficult to address using *in utero* electroporation of RNAi vectors because of the transient suppression of expression and the difficulty in transfecting a sufficient proportion of layer 2/3 neurons.

MDGA1 is also expressed by a select number of other neuronal populations as they migrate, for example basilar pontine neurons and D₁ spinal interneurons (Litwack et al., 2004), and by

inference might be involved in controlling their tangential migration. Our findings minimize the risk and provide a justification for making the investments to generate additional reagents and genetically engineered mice necessary to advance the work presented here and to explore more broadly the role of MDGA1 in neuronal migration and other aspects of neural development.

References

- Adams NC, Tomoda T, Cooper M, Dietz G, Hatten ME (2002) Mice that lack astrotactin have slowed neuronal migration. *Development* 129:965–972.
- Anton ES, Kreidberg JA, Rakic P (1999) Distinct functions of alpha3 and alpha(v) integrin receptors in neuronal migration and laminar organization of the cerebral cortex. *Neuron* 22:277–289.
- Bai J, Ramos RL, Ackman JB, Thomas AM, Lee RV, LoTurco JJ (2003) RNAi reveals doublecortin is required for radial migration in rat neocortex. *Nat Neurosci* 6:1277–1283.
- Bayer S, Altman J (1991) *Neocortical development*. New York: Raven.
- Bielas S, Higginbotham H, Koizumi H, Tanaka T, Gleeson JG (2004) Cortical neuronal migration mutants suggest separate but intersecting pathways. *Annu Rev Cell Dev Biol* 20:593–618.
- Brummelkamp TR, Bernards R, Agami R (2002) A system for stable expression of short interfering RNAs in mammalian cells. *Science* 296:550–553.
- D'Arcangelo G, Miao GG, Chen SC, Soares HD, Morgan JI, Curran T (1995) A protein related to extracellular matrix proteins deleted in the mouse mutant reeler. *Nature* 374:719–723.
- Dulabon L, Olson EC, Taglienti MG, Eisenhuth S, McGrath B, Walsh CA, Kreidberg JA, Anton ES (2000) Reelin binds alpha3beta1 integrin and inhibits neuronal migration. *Neuron* 27:33–44.
- Kriegstein AR, Noctor SC (2004) Patterns of neuronal migration in the embryonic cortex. *Trends Neurosci* 27:392–399.
- Litwack ED, Babey R, Buser R, Gesemann M, O'Leary DDM (2004) Identification and characterization of two novel brain-derived immunoglobulin superfamily members with a unique structural organization. *Mol Cell Neurosci* 25:263–274.
- Marin O, Rubenstein JL (2003) Cell migration in the forebrain. *Annu Rev Neurosci* 26:441–483.
- McEvilly RJ, de Diaz MO, Schonemann MD, Hooshmand F, Rosenfeld MG (2002) Transcriptional regulation of cortical neuron migration by POU domain factors. *Science* 295:1528–1532.
- Pak W, Hindges R, Lim YS, Pfaff SL, O'Leary DDM (2004) Magnitude of binocular vision controlled by islet-2 repression of a genetic program that specifies laterality of retinal axon pathfinding. *Cell* 119:567–578.
- Panicker AK, Buhusi M, Thelen K, Maness PF (2003) Cellular signalling mechanisms of neural cell adhesion molecules. *Front Biosci* 8:d900–d911.
- Rakic P (1972) Mode of cell migration to the superficial layers of fetal monkey neocortex. *J Comp Neurol* 145:61–83.
- Saito T, Nakatsuji N (2001) Efficient gene transfer into the embryonic mouse brain using *in vivo* electroporation. *Dev Biol* 240:237–246.
- Sugitani Y, Nakai S, Minowa O, Nishi M, Jishage K, Kawano H, Mori K, Ogawa M, Noda T (2002) Brn-1 and Brn-2 share crucial roles in the production and positioning of mouse neocortical neurons. *Genes Dev* 16:1760–1765.
- Takahashi T, Goto T, Miyama S, Nowakowski RS, Caviness Jr VS (1999) Sequence of neuron origin and neocortical laminar fate: relation to cell cycle of origin in the developing murine cerebral wall. *J Neurosci* 19:10357–10371.
- Tsai LH, Gleeson JG (2005) Nucleokinesis in neuronal migration. *Neuron* 46:383–388.
- Walsh FS, Doherty P (1997) Neural cell adhesion molecules of the immunoglobulin superfamily: role in axon growth and guidance. *Annu Rev Cell Dev Biol* 13:425–456.
- Zheng C, Heintz N, Hatten ME (1996) CNS gene encoding astrotactin, which supports neuronal migration along glial fibers. *Science* 272:417–419.

Mammalian *BarH1* Confers Commissural Neuron Identity on Dorsal Cells in the Spinal Cord

Rie Saba,^{1,2} Norio Nakatsuji,² and Tetsuichiro Saito²

¹Department of Genetics, The Graduate University for Advanced Studies, National Institute of Genetics, Mishima, Shizuoka 411-8540, Japan, and

²Department of Development and Differentiation, Institute for Frontier Medical Sciences, Kyoto University, Kyoto 606-8507, Japan

Commissural neurons in the spinal cord project their axons through the floor plate using a number of molecular interactions, such as netrins and their receptor DCC (deleted in colorectal cancer). However, the molecular cascades that control differentiation of commissural neurons are less characterized. A homeobox gene, *MBH1* (mammalian *BarH1*) was expressed specifically in a subset of dorsal cells in the developing spinal cord. Transgenic mice that carried *lacZ* and *MBH1*-flanking genome sequences demonstrated that *MBH1* was expressed by commissural neurons. To analyze the function of *MBH1*, we established an *in vivo* electroporation method for the transfer of DNA into the mouse spinal cord. Ectopic expression of *MBH1* drove dorsal cells into the fate of commissural neurons with concomitant expression of TAG-1 (transiently expressed axonal surface glycoprotein 1) and DCC. Cells ectopically expressing *MBH1* migrated to the deep dorsal horn, in which endogenous *MBH1*-positive cells accumulated. These results suggest that *MBH1* functions upstream of TAG-1 and DCC and is involved in the fate determination of commissural neurons in the spinal cord.

Key words: *MBH1*; homeobox; homeodomain; *in vivo* electroporation; TAG-1; DCC

Introduction

Commissural neurons in both vertebrates and invertebrates transfer information from one side of their bodies to the other through the midline. Molecular mechanisms regulating axon guidance of these neurons have been characterized extensively (Tessier-Lavigne and Goodman, 1996; Mueller, 1999; Kaprielian et al., 2001). Netrins and DCC (deleted in colorectal cancer) play a pivotal role in axon guidance. Some commissural neurons are generated in the developing dorsal spinal cord, in which domains of progenitor cells are specified by helix-loop-helix (HLH) transcription factors (Gowan et al., 2001). The domains are initially established by TGF- β -like signals (Liem et al., 1997) and produce several cell types, which are defined by combinatorial expression of homeobox genes (Lee and Jessell, 1999; Gross et al., 2002; Muller et al., 2002). The most dorsal cell type, dI1 (D1), is generated by an HLH factor, *MATH1* (mouse atonal homolog 1). dI1 cells and a subset of commissural neurons are lost in *MATH1* knock-out mice (Bermingham et al., 2001; Gowan et al., 2001), whereas ectopic expression of *MATH1* increases the number of dI1 cells (Gowan et al., 2001). However, the molecular cascades

that form the link between the generation of the cells and their migration–axon guidance remain to be determined.

Bar-class homeobox (*BarH*) genes function in the development of various organs. *Drosophila BarH* genes control the development of the retina (Higashijima et al., 1992a) and peripheral nervous system (Higashijima et al., 1992b). A mammalian *BarH* gene, *MBH1*, is expressed at early stages of neurogenesis and is a potential regulator of neural HLH genes in the diencephalon (Saito et al., 1998). Outside of the diencephalon, *MBH1* is expressed by postmitotic neurons in the midbrain, hindbrain, spinal cord, and retina (Saito et al., 1998, 2000). Another mammalian *BarH* gene, *MBH2/Barhl1*, is also expressed in the spinal cord (Bulfone et al., 2000; Saito et al., 2000) and suggested to be a downstream gene of *MATH1* (Bermingham et al., 2001). *Xenopus BarH* genes, *XBH1* and *XBH2*, which are orthologs of *MBH1* and *MBH2*, respectively, show distinct expression patterns (Patterson et al., 2000). Expression patterns of *MBH1* and *MBH2* are similar but not identical (Saito et al., 2000), suggesting that expression of the two genes may be controlled by different mechanisms.

In this paper, we made transgenic mice carrying *lacZ* with the *MBH1*-flanking sequences and examined the cell types of *MBH1*-expressing cells in the developing mouse spinal cord. The function of *MBH1* has been revealed using the *in vivo* electroporation method.

Materials and Methods

Generation and analysis of transgenic mice. The *MBH1*-flanking sequences were obtained by screening a 129/SvJ mouse genomic library (Stratagene, La Jolla, CA) using the entire sequence of the *MBH1* cDNA (GenBank accession number AB004056) as a probe. We made a construct that carried the *lacZ*-coding region from BGZA (Yee and Rigby, 1993; Helms et al., 2000) between the 1 kb 5' and 2.5 kb 3' sequences flanking the *MBH1*-coding region. BGZA was a gift from Dr. J. Johnson

Received Sept. 25, 2002; revised Dec. 3, 2002; accepted Dec. 18, 2002.

This work was supported in part by a grant from the Japan Society for the Promotion of Science and Grants-in-Aids for Scientific Research on Priority Areas—Neural Net Project and—Advanced Brain Science Project from Ministry of Education, Culture, Sports, Science, and Technology of Japan (T.S.). We thank Masuko Tanaka and Junko Kutsuna for their technical assistance and Dr. Takayuki Sakurai for his kind advice for generating transgenic mice. We are grateful to Drs. Thomas Jessell, Jane Johnson, Ryoichiro Kageyama, and Qiufu Ma for antibodies and plasmids. We also acknowledge the Developmental Studies Hybridoma Bank maintained by the University of Iowa (Iowa City, IA) for supply of monoclonal antibodies.

Correspondence should be addressed to Tetsuichiro Saito, Department of Development and Differentiation, Institute for Frontier Medical Sciences, Kyoto University, Shogoin, Sakyo-ku, Kyoto 606-8507. E-mail: tsaito@frontier.kyoto-u.ac.jp.

Copyright © 2003 Society for Neuroscience 0270-6474/03/231987-05\$15.00/0

(University of Texas Southwestern Medical Center, Dallas, TX). Transgenic mice were generated by standard procedures (Hogan et al., 1986) using fertilized eggs from B6C3F1 (C57BL/6 × C3H) crosses. Staged transgenic embryos were dissected in cold PBS and fixed in 4% paraformaldehyde. Whole mount 5-bromo-4-chloro-3-indolyl- β -D-galactopyranoside staining of the embryos was performed as described previously (Verma-Kurvari et al., 1996). Other constructs that carried longer *MBH1*-flanking sequences also demonstrated the same *lacZ* expression pattern as the above construct, recapitulating endogenous *MBH1* expression. After staining, the embryos were postfixed and embedded in paraffin. Microtome sections (7 μ m) were stained with Nuclear Fast Red (Vector Laboratories, Burlingame, CA). For immunostaining, fixed embryos were embedded in OCT compound and sliced at 14 μ m using a cryostat.

In vivo electroporation. *Exo utero* surgery and electroporation were performed as described previously (Saito and Nakatsuji, 2001). pCAG-EYFP (enhanced yellow fluorescent protein), which carried *EYFP* downstream of a CAG promoter (Saito and Nakatsuji, 2001), was used as a control. To express both *EYFP* and *MBH1* in the same cells, pEYFP-*MBH1* was constructed by inserting the *MBH1*-coding region downstream of the second CAG promoter of pCAG-EYFP-CAG (Saito and Nakatsuji, 2001). One microliter of DNA solution (140 nM) in PBS was injected into the central canal of the spinal cord. Five electric pulses at 22 V were delivered to the spinal cord by holding embryos with forceps-type platinum electrodes. Two kinds of electrodes, half-ring type (see Fig. 2A) and round-plate type with a 3 mm diameter (http://www.frontier.kyoto-u.ac.jp/rc01/in_vivo_electroporation.html), were used for gene transfer into the whole and a part of the spinal cord, respectively. The electric pulses were obtained from an electroporator, CUY21EDIT (Nepa Gene, Ichikawa, Japan). Survival and EYFP-positive (EYFP⁺) rates, which were calculated from surviving embryos/operated and EYFP⁺ spinal cords/surviving embryos, were 56.7 ± 4.6 and $79.9 \pm 2.7\%$, respectively. For functional analysis of genes, each result was confirmed by using another independently isolated clone with the same structure.

In situ hybridization and immunohistochemistry. *In situ* hybridization was performed as described previously (Saito et al., 1996). Antisense RNA probes were synthesized from plasmids carrying mouse cDNA clones: pMH4-1 for *MBH1* and generous gifts from Dr. T. Jessell (Columbia University, New York, NY) for *LH2B* (a LIM homeobox gene), Dr. R. Kageyama (Kyoto University, Kyoto, Japan) for *MATH1*, and Dr. Q. Ma (Harvard Medical School, Boston, MA) for *Ngn2* (neurogenin 2). Frozen sections were incubated with the following primary antibodies: 4D7 [anti-TAG-1 (transiently expressed axonal surface glycoprotein 1)], AF5 (anti-DCC; Calbiochem, La Jolla, CA), 40.2D6 [anti-Is11 (Islet-1)], 4F2 [anti-Lim1/2 (a homeodomain protein)], rabbit polyclonal L1 (anti-LH2A/B, gift from Dr. Jessell), goat anti- β -galactosidase (β -gal) (Biogenesis, Kingston, NH), and rabbit anti-GFP (Molecular Probes, Eugene, OR). 4D7, 40.2D6, and 4F2 were obtained from the Developmental Studies Hybridoma Bank (University of Iowa, Iowa City, IA). Signals were visualized by the following secondary antibodies: donkey anti-rabbit IgG, anti-mouse IgG, or anti-mouse IgM conjugated with Cy3 or FITC (Jackson ImmunoResearch, West Grove, PA); and donkey anti-goat IgG conjugated with Alexa Fluor 488 (Molecular Probes). Immunofluorescent studies were performed as described previously (Saito and Nakatsuji, 2001).

Results

MBH1 expression marked a subset of cells in the spinal cord

Expression of *MBH1* was detected in the mouse dorsal spinal cord at embryonic day 10.5 (E10.5) (Fig. 1A). At E11.5, the expression expanded ventrally to the deep dorsal horn (Fig. 1C). Later than E12.5, the expression was mainly restricted to the deep dorsal horn (Fig. 1E). The pattern of the expression during development resembled that of ventral migration of some dorsal neurons (Leber and Sanes, 1995), suggesting that *MBH1* was expressed by these migrating neurons. A stream of cells between the deep dorsal horn and the floor plate also expressed *MBH1* at E12.5 (Fig. 1E, arrows). *MBH1* expression in the ventral spinal

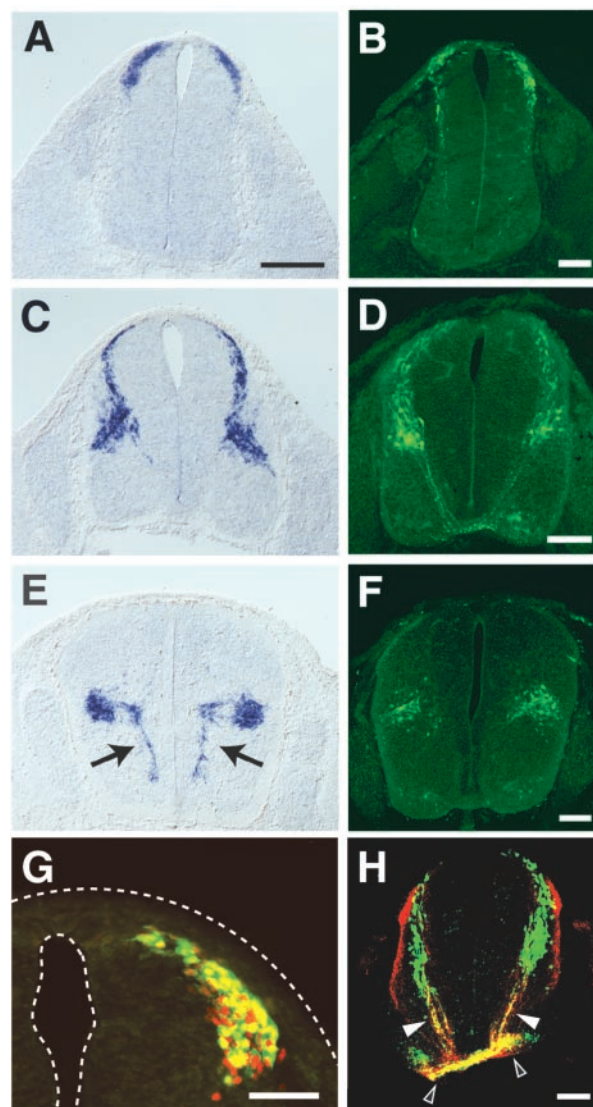


Figure 1. *MBH1* expression in the developing mouse spinal cord. Transverse sections at brachial levels of embryos at E10.5 (A, B), E11.5 (C, D) and E12.5 (E, F) were hybridized with antisense cRNA probes for *MBH1* (A, C, E) and immunostained using an anti- β -gal antibody (B, D, F). Embryos carrying the *MBH1/lacZ* transgene were used (B, D, F–H). Arrows indicate streams of *MBH1*⁺ cells between the deep dorsal horn and the floor plate. Control hybridization using a sense-strand probe of *MBH1* gave no specific signals (data not shown). Similar expression patterns of *MBH1* were observed from cervical to lumbar levels. G, Transverse section of the E10.5 spinal cord was stained with antibodies against the β -gal (green) and LH2A/B proteins (red). H, Double-label immunostaining with the anti- β -gal (green) and anti-TAG-1 (red) antibodies of the E11.5 spinal cord. Filled and open arrowheads indicate β -gal⁺ axons and ventral funiculi, respectively. Scale bars: (in A) A, C, E, 200 μ m; B, D, F–H, 100 μ m.

cord became confined to a group of cells dorsolateral to the floor plate at later stages (see Fig. 4B), suggesting that *MBH1*⁺ cells in the stream are under ventromedial migration at E12.5.

Characterization of *MBH1*-expressing cells

To examine which types of cells expressed *MBH1*, transgenic mice with *lacZ* under the control of the *MBH1*-flanking DNA sequences were generated. The transgenic mice expressed the *lacZ* product β -gal in a pattern recapitulating endogenous *MBH1* expression (Fig. 1B, D, F). Coexpression of *MBH1* and *lacZ* was confirmed by immunostaining using an anti-*MBH1* antibody (data not shown). All β -gal⁺ cells were labeled with antibodies against the LH2A/B proteins (Fig. 1G), a marker of dI1 cells, but

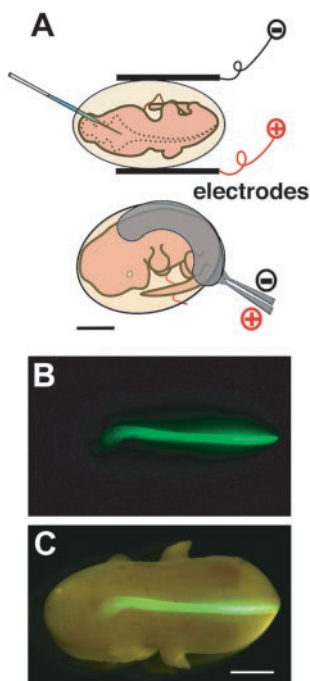


Figure 2. DNA transfer into the mouse spinal cord by *in vivo* electroporation. *A*, Schematic representation of DNA injection and electrodes. *EYFP* was introduced into the E11.5 spinal cord. *B*, Dorsal view of an embryo at E13.5, 2 d after electroporation. *C*, Semi-illuminated view of *B*. *EYFP* was expressed in only one side of the spinal cord closer to the anode. Scale bars: 2 mm.

not with antibodies against the *Isl1* and *Lim1/2* proteins (data not shown), suggesting that *MBH1* is expressed by d11 cells.

Because the β -gal protein spreads throughout the cytoplasm, it enabled us to examine the morphologies of *MBH1*⁺ cells. β -gal⁺ signals were detected in axons projecting to the floor plate and ventral funiculi (Fig. 1*H*). The β -gal⁺ axons were labeled with specific markers of commissural neurons, anti-TAG-1 and anti-DCC antibodies (Fig. 1*H*; data not shown). These results indicate that *MBH1* is expressed by commissural neurons.

In vivo electroporation into the spinal cord

To examine the function of *MBH1*, we established a system for the forced expression of a gene in the mouse spinal cord by modifying our *in vivo* electroporation method to the brain (Saito and Nakatsuji, 2001). The uterine wall was cut to see embryos clearly, and DNA was injected into the central canal of the spinal cord (Fig. 2). Then electric pulses were applied to the spinal cord using half-ring-type electrodes (Fig. 2*A*). The electrodes helped better survival of embryos by limiting electric pulses mainly onto the spinal cord. After electroporation, a reporter gene, *EYFP*, was expressed only in one side of the spinal cord (Fig. 2*B,C*).

Ectopic expression of *MBH1*

Using this system, p*EYFP-MBH1*, which carried both the *EYFP* and *MBH1* genes downstream of ubiquitous CAG promoters, was introduced into the E11.5 mouse spinal cord. At this stage, DNA will be taken up by cells that are not fated to express *MBH1* for the following two reasons: (1) endogenous *MBH1*⁺ cells are away from the ventricle (Fig. 1*C*), and (2) DNA is transferred to cells adjacent to the ventricle by this method (Saito and Nakatsuji, 2001). DNA will be also introduced mainly into dorsal cells, because the central canal is wider in the dorsal side. Transfection with *EYFP* alone as a control mostly labeled only dorsal cells, as expected (Fig. 3*A*). In contrast, more ventral *EYFP*⁺ cells were

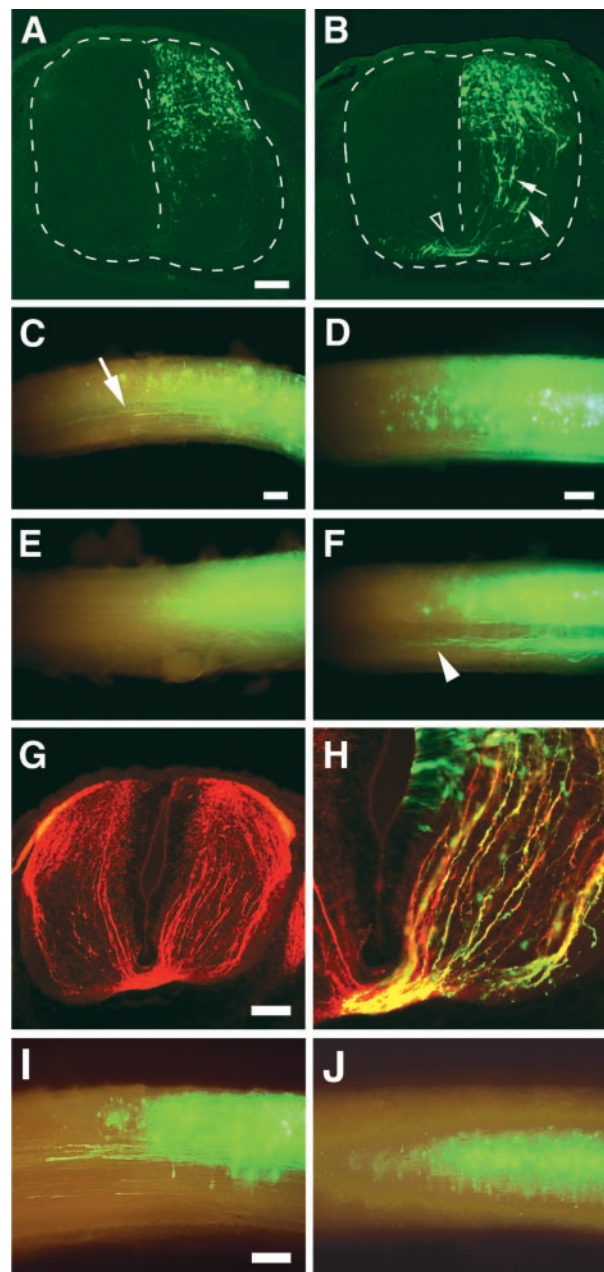


Figure 3. Generation of commissural neurons by ectopic expression of *MBH1*. E11.5 mouse spinal cords were transfected with *EYFP* alone (*A, C, E, I*) and both *EYFP* and *MBH1* (*B, D, F–H, J*). Right sides of sections were closer to the anode and transfected with these genes (*A, B, G, H*). *A, B*, Transverse sections of the spinal cord at brachial levels, 2 d after electroporation. *Arrows* and *arrowhead* indicate *EYFP*⁺ cells with morphologies similar to migratory commissural neurons and commissural axons, respectively. Similar patterns of *EYFP*⁺ cells and axons were observed through all axial levels of the spinal cord in all electroporated *EYFP*⁺ embryos ($n = 15$ for *EYFP* alone; $n = 25$ for coexpression of *EYFP* and *MBH1*). Lateral (*C, D, I, J*) and ventral (*E, F*) views of the spinal cord electroporated at lumbar levels, 3 (*C–F*) and 4 (*I, J*) d after electroporation. Rostral is to the left. *Arrow* and *arrowhead* indicate *EYFP*⁺ ipsilaterally projecting and commissural axons, respectively. *G, H*, Transverse section of the E12.5 spinal cord, 1 d after transfection with *EYFP* and *MBH1*. The section was stained with antibodies against TAG-1 (red) and GFP (green). Misexpression of either *LH2B*, a LIM homeobox gene, or *PHD1*, a paired-like homeobox gene expressed in the dorsal spinal cord (Saito et al., 1996), did not generate more commissural axons. Scale bars: (in *A, B*), 100 μ m; (in *C, E*), 200 μ m; (in *D, F*), 200 μ m; *G, H*, 100 μ m; (in *I, J*), 200 μ m.

generated by coexpression with *MBH1* (Fig. 3*B*, *arrows*). The ventral *EYFP*⁺ cells had morphologies similar to some commissural neurons (Silos-Santiago and Snider, 1992). Transfection of *MBH1* also produced more *EYFP*⁺ commissural axons (Fig. 3*B*,

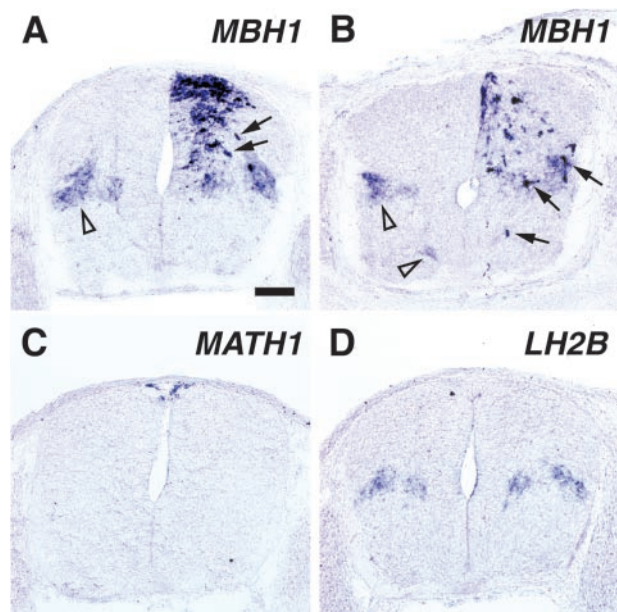


Figure 4. Comparison of *MBH1*-misexpressing cells with endogenous *MBH1*⁺ cells using *in situ* hybridization. After electroporation at E11.5, transverse sections of the mouse spinal cord were annealed with antisense cRNA probes of *MBH1* (A, B), *MATH1* (C), and *LH2B* (D). Right sides were transfected. Embryos were recovered at E12.5 (A, C, D) and at E13.5 (B). Arrowheads and arrows indicate endogenous *MBH1*⁺ domains and *MBH1*-misexpressing cells, respectively. Expression of *MATH1* and *LH2B* was not upregulated at E13.5 either (data not shown). Transfection with *EYFP* alone did not affect the expression of the genes (data not shown). Scale bar (in A): A–D, 100 μ m.

arrowhead). The cells transfected with *EYFP* alone projected ascending *EYFP*⁺ axons ipsilaterally (Fig. 3C, arrow) but not commissural axons (Fig. 3E). In contrast, cells ectopically expressing *MBH1* projected ascending commissural axons (Fig. 3F, arrowhead). Coexpression of *MBH1* and *EYFP* in the same cells was confirmed by immunostaining using the anti-*MBH1* antibody (data not shown). There were more TAG-1⁺ axons observed in the *MBH1*-transfected side (Fig. 3G). *EYFP*⁺ axons were labeled with the anti-TAG-1 antibody (Fig. 3H). Similarly, more DCC⁺ axons were generated by ectopic expression of *MBH1*, and the *EYFP*⁺ axons were also DCC⁺ (data not shown). These results indicate that the axons of the cells ectopically expressing *MBH1* had acquired molecular identities as commissural axons and that ipsilaterally projecting dorsal neurons were transfected into commissural neurons by misexpression of *MBH1*.

Migration patterns of *MBH1*-misexpressing cells

Four days after electroporation, cells expressing *EYFP* alone remained in the dorsal spinal cord (Fig. 3I). In contrast, most of *MBH1*-misexpressing cells were observed in the middle of the spinal cord (Fig. 3J), suggesting that *MBH1*-misexpressing cells may have migrated from the dorsal spinal cord. To compare *MBH1*-misexpressing cells with endogenous *MBH1*⁺ cells, *in situ* hybridization was performed (Fig. 4). At E12.5, 1 d after electroporation, more cells expressing *MBH1* were detected in the dorsal area of the *MBH1*-transfected side (Fig. 4A). Expression levels of *MBH1* were higher in the *MBH1*-misexpressing cells than those of endogenous *MBH1*, reflecting a strong activity of the CAG promoter. Those cells appeared to migrate toward the deep dorsal horn, whereas the endogenous *MBH1*⁺ cells had already settled in the deep dorsal horn at this stage (Fig. 4A, arrowhead). Two days after electroporation, many *MBH1*-misexpressing cells settled down in the deep dorsal

horn, in which the endogenous *MBH1*⁺ cells accumulated (Fig. 4B). A minor population of the *MBH1*-misexpressing cells was detected in the ventral spinal cord as well as the endogenous *MBH1*⁺ cells. These results suggest that the cells ectopically expressing *MBH1* migrate to endogenous *MBH1*⁺ domains.

Next we examined whether the misexpression of *MBH1* affects other genes. Expression of *MATH1* and *LH2B*, which are related to the differentiation of commissural neurons, was not upregulated (Fig. 4C,D; data not shown). Furthermore, no increase of LH2A/B⁺ cells was detected using the anti-LH2A/B antibody (data not shown). These findings suggest that *MATH1* and *LH2A/B* are not downstream of *MBH1*.

Discussion

Commissural neuron differentiation by *MBH1*

The results obtained by the ectopic expression of *MBH1* suggest that *MBH1* regulates at least three aspects of the differentiation of commissural neurons. Expression of TAG-1 and DCC, which are markers of commissural neurons, were induced by *MBH1*. Because DCC is a receptor of netrins, the ectopic expression of DCC may be responsible for axon projection of the *MBH1*-misexpressing cells to the floor plate. Their axons elongated along the floor plate after crossing it, as do endogenous commissural neurons. The *MBH1*-misexpressing cells appeared to migrate to the endogenous *MBH1*⁺ domains. These findings suggest that several genes involved in the differentiation of commissural neurons are regulated downstream of *MBH1*.

There are several types of commissural neurons at various dorsoventral domains in the spinal cord. Only two domains were *MBH1*⁺, showing that *MBH1* is expressed by a subset of commissural neurons. The expression of *MBH1* at E10.5, which was restricted to the dorsal edge of the spinal cord, was similar to that of *MATH1*, but the expression of *MATH1* was limited to the ventricular zone and detected at E9.5 (Helms and Johnson, 1998; data not shown), earlier than that of *MBH1*. All β -gal⁺ cells of the *MBH1/lacZ* transgenic embryos expressed LH2A/B, which is a marker of dI1 cells and expressed downstream of *MATH1*. These results indicate that *MBH1* is expressed in a lineage of cells that have expressed *MATH1*. All LH2A/B⁺ cells, however, appeared not to be β -gal⁺, suggesting that *MBH1* is expressed in a subset of LH2A/B⁺ cells. The expression patterns of *MBH1* were similar to those of *LH2B* in the spinal cord (Fig. 4; data not shown), suggesting that *MBH1* may be expressed in the same lineage of cells that express *LH2B*.

Misexpression of *MBH1* generated more commissural neurons without induction of LH2A/B, suggesting that LH2A/B may not exert the same function as *MBH1* in the differentiation of commissural neurons. This was confirmed by ectopic expression of *LH2B* in the spinal cord, which did not produce more commissural neurons (data not shown). On the other hand, misexpression of *MATH1* generated more commissural neurons (data not shown), suggesting that *MATH1* is upstream of *MBH1*. At E11.5, the domain of *MBH1* expression closely resembled the β -gal⁺ domain of transgenic mice that carried *lacZ* under the control of *MATH1*-flanking sequences (Helms and Johnson, 1998). Moreover, the 3' *MBH1*-flanking sequence used for the transgenic mice in this study contained an E-box (CAGCTG), which could bind the *MATH1* protein (Akazawa et al., 1995; Helms et al., 2000). These findings suggest that *MBH1* may be a downstream target of the *MATH1* protein.

A recent report has shown that excess commissural neurons were generated in *Lbx1* (a *Ladybird*-like homeobox gene 1) mutant mice because of mis-specification of dorsal interneurons (Gross

et al., 2002). This is similar to our results from the misexpression of *MBH1*. However, expression of *Isl1* and *Lim1/2*, which are affected in the mutant mice, were not perturbed by the misexpression of *MBH1* (data not shown). This result suggests that *MBH1* generates ectopic commissural neurons independently of a transcriptional cascade exerted in the *Lbx1* mutant mice.

Regulation of cell migration by *MBH1*

The transgenic mice carrying *lacZ* with the *MBH1*-flanking sequences visualized *MBH1*⁺ cells. At E10.5 and E11.5, the stages when the *MBH1*⁺ cells were located between the dorsal edge and the deep dorsal horn in the spinal cord, they showed morphologies typical of some migratory neurons (unipolar with leading processes) (Leber and Sanes, 1995). Together with expression patterns of *MBH1*, this suggests that *MBH1* is expressed during the migration of commissural neurons. The endogenous *MBH1*⁺ cells migrated to the deep dorsal horn along the marginal zone of the spinal cord. In contrast, *MBH1*-misexpressing cells appeared not to follow the same route as the endogenous *MBH1*⁺ cells but rather to take a direct shortcut route from their birthplaces in the ventricular zone to the deep dorsal horn. These observations suggest that *MBH1* may instruct the cells where to migrate, responding to an extracellular factor in the spinal cord. The factor may be released from the deep dorsal horn to attract the cells or may exclude the cells from the dorsolateral region of the spinal cord.

MBH1 was also expressed by granule cells during their migration in the developing cerebellum (Saito et al., 2000). *MATH1*, *TAG-1*, and *DCC* are all expressed in the developing cerebellum as well (Yamamoto et al., 1990; Akazawa et al., 1995; Livesey and Hunt, 1997), suggesting that there is a common cascade of genes between commissural neurons and the cerebellum.

Various functions of *BarH* genes

Some commissural neurons are generated downstream of *Ngn2* (Simmons et al., 2001). We showed that forced expression of *MBH1* upregulates *Ngn2* in P19 cells, reflecting expression patterns of the two genes in the developing diencephalon (Saito et al., 1998). *Ngn2* was not activated by ectopic expression of *MBH1* in the developing spinal cord (data not shown). *MBH1* requires another unknown factor that is transiently expressed in P19 cells to upregulate *Ngn2* (Saito et al., 1998). The factor may have been absent in the spinal cord at the stage when *MBH1* was ectopically expressed. *MBH1* was expressed in mitotically active cells in the ventricular zone of the diencephalon, whereas postmitotic cells expressed *MBH1* in the spinal cord. *MBH1* may have different functions at different stages of neurogenesis. Similarly, *Drosophila BarH* genes show various functions (Higashijima et al., 1992a,b).

In vivo electroporation in mouse

Both gain- and loss-of-function analyses are essential to establish gene function. Gene knock-out techniques have enabled the loss-of-function analysis of many genes in mouse. On the other hand, gain-of-function approaches have been used extensively in chick. The genes and gene combinations that regulate some stages of development are not exactly the same between chick and mouse. This report demonstrates that the *in vivo* electroporation technique is a powerful tool to reveal gene function in the mouse. This technique will greatly facilitate functional analyses of genes, because it may also be applied to knock-out and transgenic mice.

References

Akazawa C, Ishibashi M, Shimizu C, Nakanishi S, Kageyama R (1995) A mammalian helix-loop-helix factor structurally related to the product of *Drosophila* proneural gene *atonal* is a positive transcriptional regulator expressed in the developing nervous system. *J Biol Chem* 270:8730–8733.

Birmingham NA, Hassan BA, Wang VY, Fernandez M, Banfi S, Bellen HJ, Fritsch B, Zoghbi HY (2001) Proprioceptor pathway development is dependent on *MATH1*. *Neuron* 30:411–422.

Bulfone A, Menguzzato E, Broccoli V, Marchitello A, Gattuso C, Mariani M, Consalez GG, Martinez S, Ballabio A, Banfi S (2000) *Barhl1*, a gene belonging to a new subfamily of mammalian homeobox genes, is expressed in migrating neurons of the CNS. *Hum Mol Genet* 9:1443–1452.

Gowan K, Helms AW, Hunsaker TL, Collisson T, Ebert PJ, Odom R, Johnson JE (2001) Crossinhibitory activities of *Ngn1* and *Math1* allow specification of distinct dorsal interneurons. *Neuron* 31:219–232.

Gross MK, Dottori M, Goulding M (2002) *Lbx1* specifies somatosensory association interneurons in the dorsal spinal cord. *Neuron* 34:535–549.

Helms AW, Johnson JE (1998) Progenitors of dorsal commissural interneurons are defined by *MATH1* expression. *Development* 125:919–928.

Helms AW, Abney AL, Ben-Arie N, Zoghbi HY, Johnson JE (2000) Autoregulation and multiple enhancers control *Math1* expression in the developing nervous system. *Development* 127:1185–1196.

Higashijima S, Kojima T, Michiue T, Ishimaru S, Emori Y, Saigo K (1992a) Dual *Bar* homeobox genes of *Drosophila* required in two photoreceptor cells, R1 and R6, and primary pigment cells for normal eye development. *Genes Dev* 6:50–60.

Higashijima S, Michiue T, Emori Y, Saigo K (1992b) Subtype determination of *Drosophila* embryonic external sensory organs by redundant homeobox genes *BarH1* and *BarH2*. *Genes Dev* 6:1005–1018.

Hogan B, Constantini F, Lacy E (1986) Manipulating the mouse embryo: a laboratory manual, pp 79–203. Cold Spring Harbor, NY: Cold Spring Harbor Laboratory.

Kaprielian Z, Runko E, Imondi R (2001) Axon guidance at the midline choice point. *Dev Dyn* 221:154–181.

Leber SM, Sanes JR (1995) Migratory paths of neurons and glia in embryonic chick spinal cord. *J Neurosci* 15:1236–1248.

Lee KJ, Jessell TM (1999) The specification of dorsal cell fates in the vertebrate central nervous system. *Annu Rev Neurosci* 22:261–294.

Liem Jr KF, Tremml G, Jessell TM (1997) A role for the roof plate and its resident TGF β -related proteins in neuronal patterning in the dorsal spinal cord. *Cell* 91:127–138.

Livesey FJ, Hunt SP (1997) Netrin and netrin receptor expression in the embryonic mammalian nervous system suggests roles in retinal, striatal, nigral, and cerebellar development. *Mol Cell Neurosci* 8:417–429.

Mueller BK (1999) Growth cone guidance: first steps towards a deeper understanding. *Annu Rev Neurosci* 22:351–388.

Muller T, Brohmann H, Pierani A, Heppenstall PA, Lewin GR, Jessell TM, Birchmeier C (2002) The homeodomain factor *Lbx1* distinguishes two major programs of neuronal differentiation in the dorsal spinal cord. *Neuron* 34:551–562.

Patterson KD, Cleaver O, Gerber WV, White FG, Krieg PA (2000) Distinct expression patterns for two *Xenopus Bar* homeobox genes. *Dev Genes Evol* 210:140–144.

Saito T, Nakatsuji N (2001) Efficient gene transfer into the embryonic mouse brain using *in vivo* electroporation. *Dev Biol* 240:237–246.

Saito T, Lo L, Anderson DJ, Mikoshiba K (1996) Identification of novel paired homeodomain protein related to *C. elegans unc-4* as a potential downstream target of *MASH1*. *Dev Biol* 180:143–155.

Saito T, Sawamoto K, Okano H, Anderson DJ, Mikoshiba K (1998) Mammalian *BarH* homologue is a potential regulator of neural bHLH genes. *Dev Biol* 199:216–225.

Saito T, Hama T, Saba R, Nakatsuji N (2000) Mammalian *Bar*-class homeobox genes. *Soc Neurosci Abstr* 26:600.21.

Silos-Santiago I, Snider WD (1992) Development of commissural neurons in the embryonic rat spinal cord. *J Comp Neurol* 325:514–526.

Simmons AD, Horton S, Abney AL, Johnson JE (2001) *Neurogenin2* expression in ventral and dorsal spinal neural tube progenitor cells is regulated by distinct enhancers. *Dev Biol* 229:327–339.

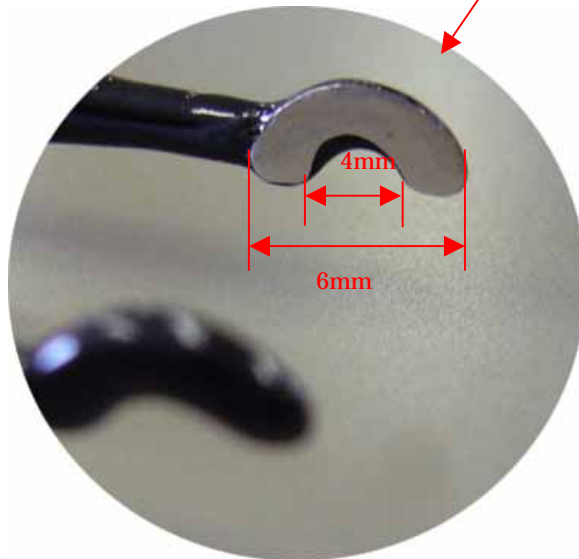
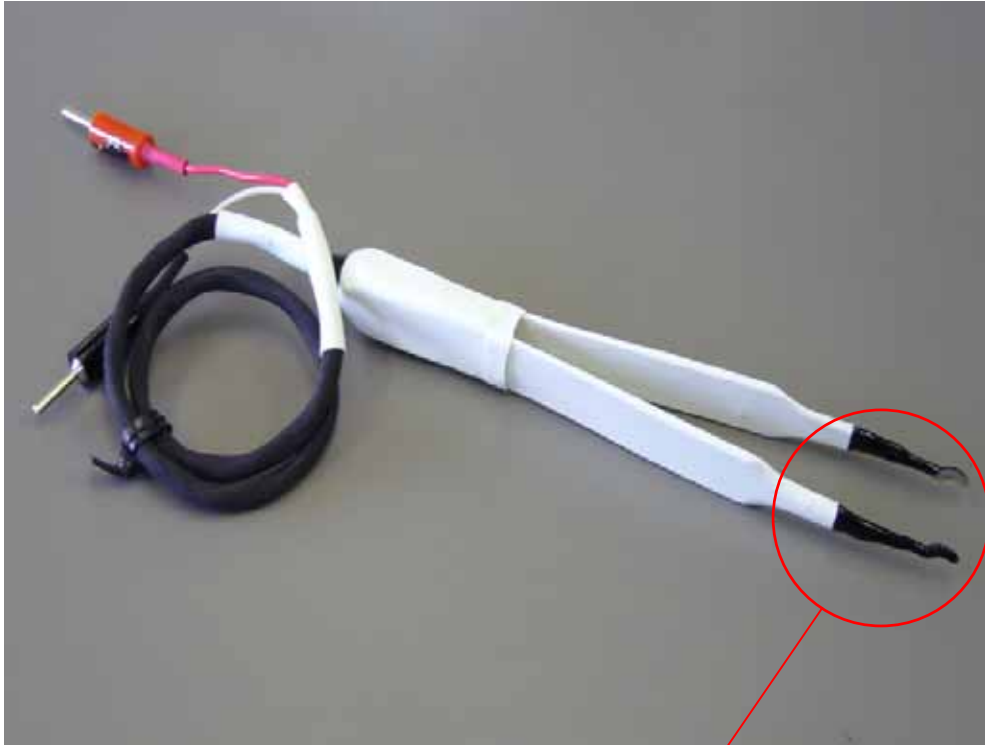
Tessier-Lavigne M, Goodman CS (1996) The molecular biology of axon guidance. *Science* 274:1123–1133.

Verma-Kurvari S, Savage T, Gowan K, Johnson JE (1996) Lineage-specific regulation of the neural differentiation gene. *MASH1*. *Dev Biol* 180:605–617.

Yamamoto M, Hassinger L, Crandall JE (1990) Ultrastructural localization of stage-specific neurite-associated proteins in the developing rat cerebral and cerebellar cortices. *J Neurocytol* 19:619–627.

Yee SP, Rigby PWJ (1993) The regulation of myogenin gene expression during the embryonic development of the mouse. *Genes Dev* 7:1277–1289.

CUY651
For spinal cord of mouse embryo



In utero electroporation parameter

Stage	Diameter	Electrode	Voltage	Pulse length	Pulse interval	Cycles	Current
E12.5	3mm	CUY650P3	33V	30 msec.	970 msec.	4	30-60mA
E13.5	5mm	CUY650P5	30V	50 msec.	950 msec.	4	30-60mA
E14.5	5mm	CUY650P5	33V	50 msec.	950 msec.	4	30-60mA
E15	5mm	CUY650P5	35V	50 msec.	950 msec.	4	30-60mA

Electrodes

CUY650P1, P3

Tweezers w/Variable Gap 2 Round Platinum Plate Electrode

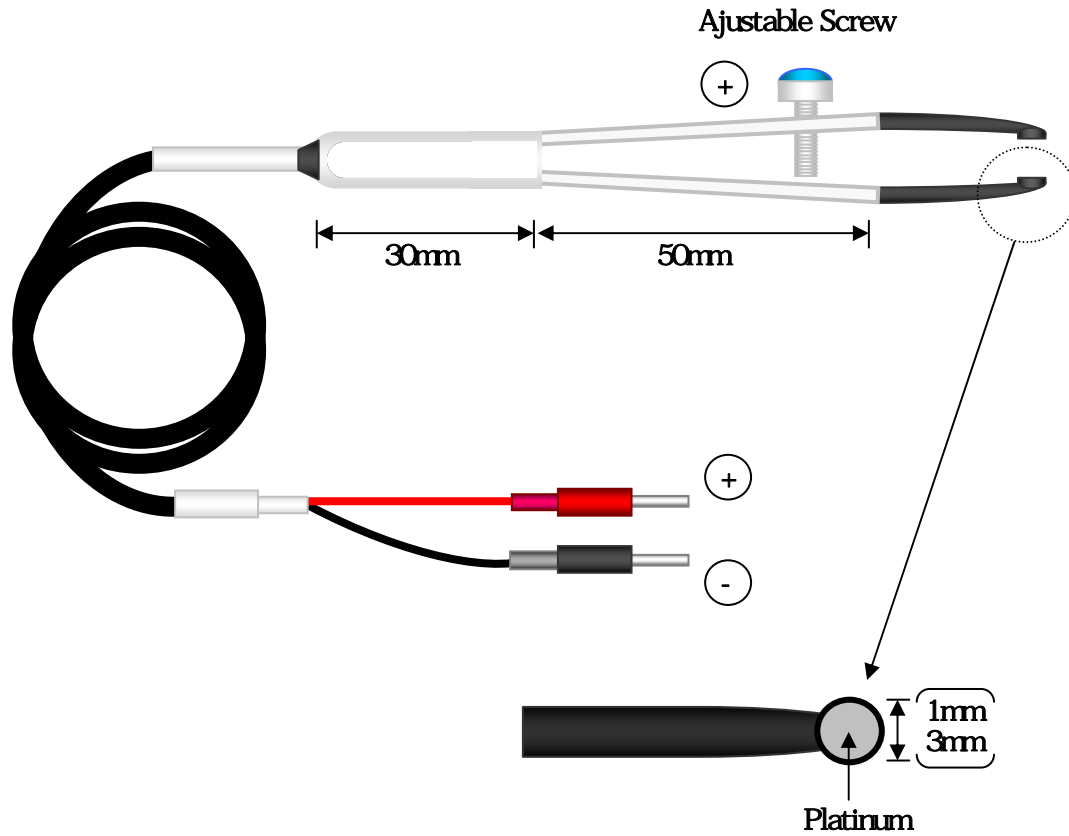
CUY650P1: 1mm diameter

CUY650P3: 3mm diameter

For Mouse Brain in Utero

For All Animal Tissues (Muscle, Skin, Bladder, Testis and Organs of Mouse, Rat,

Rabbit & Dog)



Electrodes

CUY650-5, P5, 7, P7

Tweezers w/Variable Gap 2 Round Plate Electrode

CUY650-5: Stainless Steel, 5mm diameter

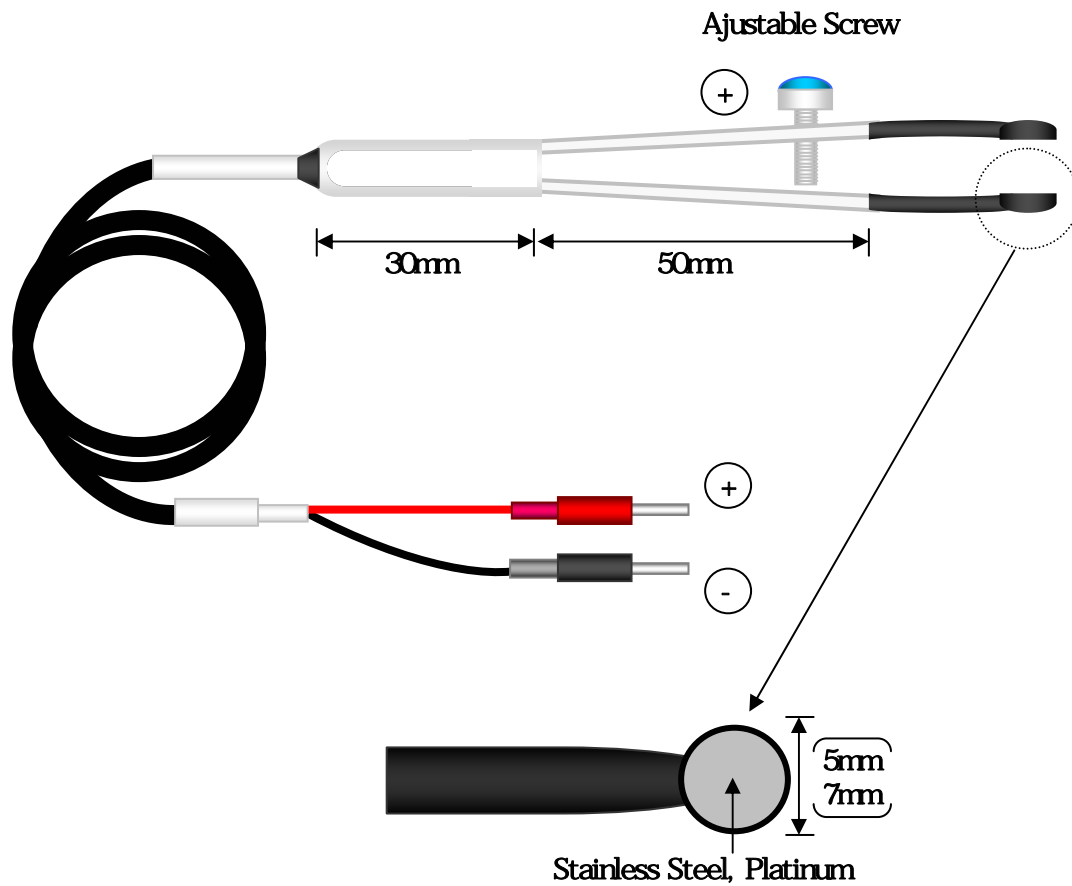
CUY650P5: Platinum, 5mm diameter

CUY650-7: Stainless Steel, 7mm diameter

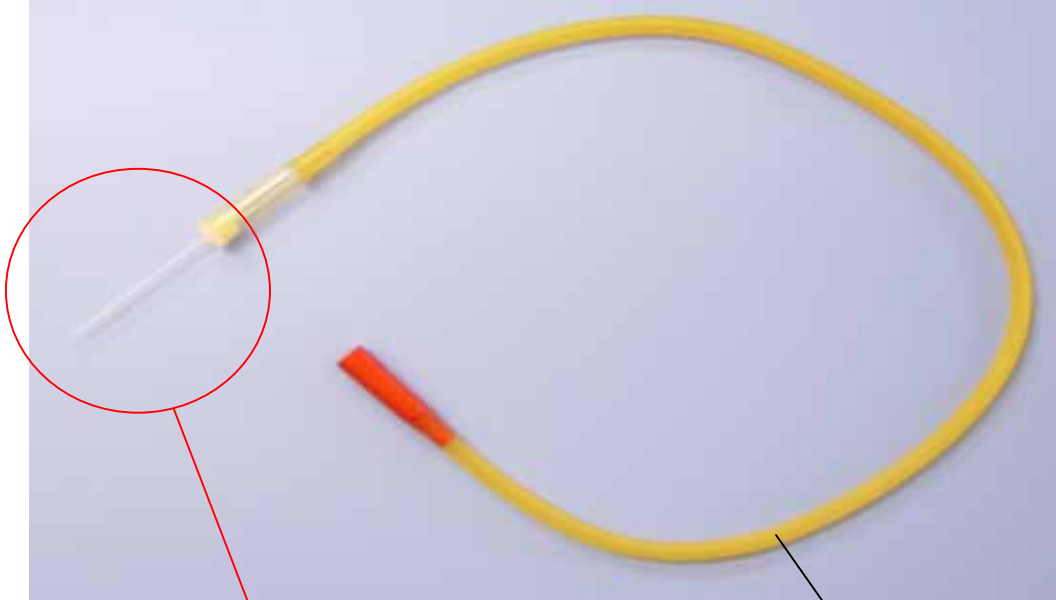
CUY650P7: Platinum, 7mm diameter

For Mouse Brain in Utero

For All Animal Tissues (Muscle, Skin, Bladder, Testis, Liver and Organs of Mouse, Rat, Rabbit & Dog)



Mouth-controlled micropipette system



Drummond scientific company



Glass capillary GD-1 (Narishge)

*** Puller PC-10 (Narishge) is required.**